



# Ozone Impacts of Gas-Aerosol Uptake in Global Chemistry Transport Models

Scarlet Stadtler<sup>1</sup>, David Simpson<sup>2,3</sup>, Sabine Schröder<sup>1</sup>, Domenico Taraborrelli<sup>1</sup>, Andreas Bott<sup>4</sup>, and Martin Schultz<sup>1</sup>

<sup>1</sup>Institut für Energie- und Klimaforschung, IEK-8, Forschungszentrum Jülich, Germany

<sup>2</sup>EMEP MSC-W, Norwegian Meteorological Institute, Oslo, Norway

<sup>3</sup>Dept. Space, Earth & Environment, Chalmers University of Technology, Gothenburg, Sweden

<sup>4</sup>Meteorological Institute University Bonn, Bonn, Germany

Correspondence to: David Simpson ([david.simpson@met.no](mailto:david.simpson@met.no))

## Abstract.

The impact of six heterogeneous gas-aerosol uptake reactions on tropospheric ozone and nitrogen species was studied using two chemical transport models, EMEP MSC-W and ECHAM-HAMMOZ. Species undergoing heterogeneous reactions in both models include  $\text{N}_2\text{O}_5$ ,  $\text{NO}_3$ ,  $\text{NO}_2$ ,  $\text{O}_3$ ,  $\text{HNO}_3$  and  $\text{HO}_2$ . Since heterogeneous reactions take place at the aerosol surface area, the modeled surface area density  $S_a$  of both models was compared to a satellite product retrieving the surface area. This comparison shows a good agreement in global pattern and especially the capability of both models to capture the extreme aerosol loadings in East Asia.

The impact of the heterogeneous reactions was evaluated by the simulation of a reference run containing all heterogeneous reactions and several sensitivity runs. One reaction was turned off in each sensitivity run to compare it with the reference run. The analysis of the sensitivity runs confirms that the globally most important heterogeneous reaction is the one of  $\text{N}_2\text{O}_5$ . Nevertheless,  $\text{NO}_2$ ,  $\text{HNO}_3$  and  $\text{HO}_2$  heterogeneous reaction gain relevance particularly in East Asia due to the presence of high  $\text{NO}_x$  concentrations and high  $S_a$  in the same region, although ECHAM-HAMMOZ showed much stronger responses than EMEP in this respect. The heterogeneous reaction of  $\text{O}_3$  itself on dust is of minor relevance compared to the other heterogeneous reactions. The impacts of the  $\text{N}_2\text{O}_5$  reactions show strong seasonal variations, with biggest impacts on  $\text{O}_3$  in spring time when photochemical reactions are active and  $\text{N}_2\text{O}_5$  levels still high. Evaluation of the models with northern hemispheric ozone surface observations yields a better agreement of the models with observations in terms of concentration levels, variability, and temporal correlations at most sites when the heterogeneous reactions are incorporated.

## 1 Introduction

Nitrogen species, ozone and atmospheric aerosols are major pollutants in the atmosphere, having strong impacts on ecosystems and human health, and also interacting with climate (Ainsworth et al., 2012; Harrison and Yin, 2000; Simpson et al., 2014; IPCC, 2013). In regions, where gas phase and aerosol pollutants meet, heterogeneous chemistry can play a significant role (Jacob, 2000). The first heterogeneous process to become prominent in atmospheric chemistry was the heterogeneous destruction



of stratospheric ozone on polar stratospheric clouds (Solomon, 1999). However, heterogeneous processes are also relevant in the lower atmosphere, influencing tropospheric ozone and therefore oxidation capacity of the atmosphere (Pöschl, 2005; Seinfeld and Pandis, 2012). An important example is the heterogeneous reaction of  $\text{N}_2\text{O}_5$  on aerosols, which is known to impact the  $\text{NO}_x$ - $\text{O}_3$  cycle while mainly removing  $\text{NO}_x$  from the troposphere (Mozurkewich and Calvert, 1988; Dentener and Crutzen, 1993; Evans and Jacob, 2005; Chang et al., 2011b; Brown and Stutz, 2012), which can lead to ozone reduction (Macintyre and Evans, 2010). Other oxidised nitrogen species also undergo heterogeneous reactions on different aerosol types.  $\text{NO}_2$ ,  $\text{HNO}_3$  and  $\text{NO}_3$  react on wet surfaces of different aerosol types and increase aerosol nitrate content (Rudich et al., 1998; Goodman et al., 1999).  $\text{HNO}_3$  reacts also with dust and sea salt particles which is again a sink for  $\text{NO}_x$  and a source for particulate nitrate (Davies and Cox, 1998; Hanisch and Crowley, 2001). Moreover, heterogeneous reaction of  $\text{NO}_2$  produces HONO which plays the role of a reservoir specie for NO and OH production (Platt et al., 1980). Other species also undergo heterogeneous reactions.  $\text{O}_3$  reacts on dust particles and this has been estimated to lead to an ozone loss of about 20% in dusty regions (Usher et al., 2003).  $\text{HO}_2$  reacts on wet particles leading to  $\text{H}_2\text{O}_2$  production (Thornton and Abbatt, 2005). Furthermore, heterogeneous reactions lead to halogen release from sea salt aerosols (Frenzel et al., 1998; Yang et al., 2008; Lowe et al., 2011). Many modeling studies have been conducted over the years on these processes, but usually heterogeneous reactions were studied individually, and typically considering annual global budgets rather than detailed temporal or spatial resolution of the impacts (Dentener and Crutzen, 1993; Rudich et al., 1998; Saathoff et al., 2001; Bauer et al., 2004; Hodzic et al., 2006; Thornton et al., 2008; Chang et al., 2011b).

This paper presents estimates of the global impact of heterogeneous reactions of  $\text{N}_2\text{O}_5$ ,  $\text{NO}_3$ ,  $\text{NO}_2$ ,  $\text{HNO}_3$ ,  $\text{HO}_2$  and  $\text{O}_3$  and evaluates each reaction in a systematic way. The influence of each reaction on the magnitude and spatial and temporal variation in surface ozone is illustrated. The greatest impacts are seen in northern hemispheric regions of North America, Europe, South and East Asia. The  $\text{N}_2\text{O}_5$  reaction is shown to significantly affect the spring-peak of surface  $\text{O}_3$  at sites in all these regions. Although the impact of  $\text{N}_2\text{O}_5$  reaction on  $\text{O}_3$  is analysed, due to technical limitations in both models no  $\text{ClNO}_2$  chemistry is included, which could decrease the impact of  $\text{N}_2\text{O}_5$  on  $\text{O}_3$ , since it is a competing  $\text{NO}_x$  loss process.

Section 2 presents the two global scale chemical transport models, EMEP MSC-W and ECHAM-HAMMOZ, as well as details of the reaction parameterisations and sensitivity tests. In section 3 a short review of the range of reaction probabilities for each heterogeneous reaction is given. Model setups and sensitivity runs are described in section 4. Section 5 first presents a comparison of the simulated surface area from the models with satellite derived product, since the surface area of aerosols is crucial for heterogeneous chemistry. Especially in polluted regions where high trace gas concentrations meet large surface areas provided by aerosols heterogeneous chemistry might be of significant importance explaining aerosol composition and trace gas mixing ratios (Jacob, 2000; Pathak et al., 2009). Furthermore, section 5 presents the results of the sensitivity tests, and comparisons of daily maximum ozone time series for 2012 with surface station observations for selected sites. Finally, section 6 summarizes the results and implications for atmospheric chemistry.



## 2 Model description

Two models, the chemical transport model EMEP MSC-W (v4.14) (Simpson et al., 2012, 2017) and the global chemistry  
5 aerosol climate model ECHAM6.3-HAM2.3MOZ1.0 (Schultz et al., in preparation) were used to study the heterogeneous  
chemistry of various compounds in the atmosphere.

### 2.1 EMEP

The EMEP MSC-W chemical transport model has been described in detail by Simpson et al. (2012), but substantial updates  
were made in the treatment of aerosols, biogenic emissions and chemistry in recent years, see Simpson et al. (2015, 2017) (and  
10 refs therein). The default model setup includes 20 vertical layers up to 100 hPa, using terrain-following coordinates, and the  
lowest layer has a thickness of about 90 m. Although originally designed for European applications (previously using a grid of  
resolution 50 km, more recently 28 km), the model is very flexible and is now applied on scales ranging from global (Jonson  
et al., 2010) to local (1-7 km grids), e.g. Vieno et al. (2010, 2014), Schaap et al. (2015). Anthropogenic emissions from land-  
based sources are here taken from the so-called PANHAM database from the EU PANDA project (<http://panda-project.eu>),  
15 which combined emissions from the global HTAP data base ([http://edgar.jrc.ec.europa.eu/htap\\_v2/index.php?SECURE=123](http://edgar.jrc.ec.europa.eu/htap_v2/index.php?SECURE=123))  
with the MIEC database for China (<http://www.meicmodel.org/>).

Emissions of VOC from biogenic sources are calculated in the model based upon land-cover and meteorological conditions.  
Emission factors for earlier versions of the EMEP model were mainly intended for European simulations (Simpson et al., 1999,  
2012), but during 2016-2017 the factors used in non-European areas were substantially revised - see Simpson et al. (2017) for  
20 details. For details of other emissions (soil-NO, lightning, aircraft, biomass-burning), see Simpson et al. (2012). For the present  
study meteorological data from the European Centre for Medium Range Weather Forecasting Integrated Forecasting System  
(ECMWF-IFS) model (<http://www.ecmwf.int/research/ifsdocs/>) were used, and the model runs with  $1 \times 1^\circ$  latitude-longitude  
resolution.

The chemical scheme in the EMEP MSC-W model, denoted 'EmChem16', consists of a standard gas-phase mechanism  
25 (132 species, 183 reactions, a recent update of the earlier EmChem03 evaluated by Andersson-Sköld and Simpson 1999),  
extended with organic aerosols using a volatility-basis-set scheme (Bergström et al., 2012; Simpson et al., 2012), plus sea-salt  
(Tsyro et al., 2011) and dust aerosol. Unlike ECHAM-HAMMOZ, the EMEP model includes  $\text{NH}_3$  and handles the resulting  
interactions with sulphate,  $\text{HNO}_3$  and ammonium-nitrate through the use of the MARS equilibrium solver (Binkowski and  
Shankar, 1995). Unfortunately, interactions with sea-salt have not yet been implemented in EMEP-MARS. The chemical  
30 equations are solved using the TWOSTEP algorithm (Verwer and Simpson, 1995; Verwer et al., 1996).

The EMEP MSC-W model has been extensively compared with measurements of many different compounds with generally  
good performance (e.g. Simpson et al., 2006a, b; Fagerli and Aas, 2008; Aas et al., 2012; Gauss et al., 2011), although most  
of these studies have focused on Europe. Still, in comparisons with global data and other models, the EMEP MSC-W model  
seems to perform well, especially more recent versions (Jonson et al., 2010, 2015; Angelbratt et al., 2011; Bian et al., 2017).



As of EMEP MSC-W model version rv4.7 (Simpson et al., 2015), aerosol surface area ( $S_a$ ) is estimated using the empirical relations of Gerber (1985), which simply requires aerosol mass concentrations and assumed aerosol density and size-parameters. Values of  $S_a$  are calculated for fine and coarse particulate matter ( $PM_f$ ,  $PM_c$ ) both as totals (including all components, for reaction R1-3,5 in Table 1), and separately for coarse sea-salt and dust particles - which we denote as  $S_{ss}$  and  $S_{du}$  respectively. The distinction between total area  $S$  and  $S_{ss}$  and  $S_{du}$  was made to allow the use of Gerber's specific parameterizations for sea-salt and dust for reactions R5 and R6 (Table 1), with the assumption that where concentrations are large (eg over oceans, deserts) these give a better estimate of  $S$  than the rural parameterisation would give. Further, for  $S_{du}$  the aerosol is assumed to be dry; which is not always true but is intended to reflect the nature of desert dust dominated aerosol. The EMEP model does not include fine-mode formation of  $NO_3^-$  through reaction R4, since the relationship between  $HNO_3$  and fine-mode nitrate is given by the thermodynamic equilibrium solver MARS.

## 2.2 ECHAM-HAMMOZ

ECHAM-HAMMOZ is an aerosol chemistry climate model capable of performing interactive aerosol chemistry simulations. For this study simulations were done using version ECHAM6.3-HAM2.3MOZ1.0 (<https://redmine.hammoz.ethz.ch/projects/hammoz/wiki/Echam630-ham23-moz10>). The model system ECHAM-HAMMOZ consists of the general circulation model ECHAM6.3 (Stevens et al., 2013), the aerosol model HAM2.3 (Neubauer et al., in preparation; Zhang et al., 2012) and the chemistry model MOZ1.0 (Schultz et al., in preparation). ECHAM calculates meteorological variables, cloud processes and radiative transfer considering greenhouse gases and aerosols. The simulations in this study make use hybrid sigma coordinates with 47 vertical layers, while the surface layer thickness is about 50 m. The horizontal resolution T63 leads to an associated  $1.875^\circ \times 1.875^\circ$  Gaussian grid.

HAM simulates the evolution of aerosols considering aerosol and aerosol precursor emissions, microphysical processes as nucleation, coagulation, accumulation, sedimentation, dry and wet deposition. Via direct and indirect aerosol effects a feedback to climate system is simulated (Neubauer et al., in preparation). The aerosols in HAM are assumed to be internally mixed and consist of up to 5 components: sulphate, sea salt, dust, organic carbon and black carbon. To describe the aerosol number the microphysical driver M7 uses distribution seven log normal functions describing four wet aerosol modes and three dry aerosol modes. Hence, the wet functions cover nucleation, Aitken, accumulation, and coarse modes and the dry functions do not cover the nucleation mode. The height and median radius of the distribution are calculated, just its width is fixed. Due to aerosol aging it is possible for insoluble particles to become soluble (Vignati et al., 2004). Dust and sea salt emissions are interactively calculated considering the wind speed at 10 m. Dimethylsulphate emissions are parametrized and emissions of sulphate dioxide, sulphate aerosol, black carbon and organic carbon are taken from the Representative Concentration Pathway (RCP) 8.5 emissions (Van Vuuren et al., 2011). Finally, optical properties of the aerosol are calculated and impact the atmospheric circulation in ECHAM (Zhang et al., 2012).

Atmospheric chemistry is simulated by MOZ which is based on MOZART3.5 (Model for Ozone and Related chemical Tracers version 3.5) (Stein et al., 2012) connecting tropospheric chemistry of MOZART4 (Emmons et al., 2010) and stratospheric chemistry of MOZART3 (Kinnison et al., 2007). Further development since Stein et al. (2012) lead to MOZ being a chemical



mechanism resembling to CAM-chem (Community Atmosphere Model with Chemistry) (Lamarque et al., 2012) with several revisions, extended chemistry of aromatic compounds and a more detailed isoprene chemistry based on Taraborrelli et al. (2009). The version MOZ1.0 used here consists of 242 tracers, 733 chemical reactions which contain 142 photolysis reactions, 6 heterogeneous tropospheric reactions and 16 stratospheric heterogeneous reactions. Further, MOZ calculates dry and wet deposition of gases. Anthropogenic emissions are taken from the emission inventory RCP 8.5 (Van Vuuren et al., 2011). Biogenic emissions of VOC and NO<sub>2</sub> are calculated interactively by MEGAN (Model of Emissions of Gases and Aerosols from Nature) (Guenther et al., 2006; Henrot et al., 2017). NO lightning emission are parametrized as described by Grewe et al. (2001).

HAM and MOZ interact via two physical processes. First, assuming spherical aerosols, the surface area density for heterogeneous reactions is calculated using aerosol distribution and median radius. Second, MOZ provides fields of oxidants for aerosol formation from gas-phase precursors. The HAMMOZ coupling does not include ammonium nitrate formation due to the lack of nitrate aerosol in the current HAM version. Therefore, reactive uptake of nitric acid leads to a total loss, based on the assumption of a quick loss of gas phase HNO<sub>3</sub> and particulate nitrate. To underline, heterogeneous reactions in ECHAM-HAMMOZ do not form HNO<sub>3</sub> in the gas phase, but introduce a direct loss to the products HNO<sub>3</sub> and NO<sub>3</sub><sup>-</sup>.

### 3 Heterogeneous reactive uptake

Experimental studies show that oxidised nitrogen species, ozone and the hydroperoxy radical undergo heterogeneous reactions on wet and dry aerosols. Heterogeneous reactions can be modeled as a pseudo-first order process (Ammann et al., 2013).

$$\frac{d[X]_g}{dt} = -k_X[X]_g \quad (1)$$

The change in gas phase concentration of the species X = N<sub>2</sub>O<sub>5</sub>, NO<sub>3</sub>, NO<sub>2</sub>, HNO<sub>3</sub>, HO<sub>2</sub>, O<sub>3</sub> is proportional to its gas phase concentration [X]<sub>g</sub> and a reaction rate coefficient k<sub>X</sub> (Schwartz, 1986)

$$k_X = \left( \frac{r_p}{D_g} + \frac{4}{c_X \cdot \gamma_X} \right)^{-1} S_a \quad (2)$$

where D<sub>g</sub> represents the gas phase diffusion coefficient, r<sub>p</sub> is the particle radius, c<sub>X</sub> is the mean molecular velocity of the species X, γ<sub>X</sub> represents the reaction probability and S<sub>a</sub> the surface area density. The γ<sub>X</sub> values are generally determined from laboratory measurements. The first term in Eqn. 2 is very small for particles of accumulation mode and larger, and is neglected in the EMEP model. The main challenges for chemistry transport models are the calculation of a proper surface area density S<sub>a</sub> and the parametrization of the reaction probability γ<sub>X</sub>.

First, Table 1 summarizes the heterogeneous reactions investigated in this study. Second, sections 3.1-3.6 discuss literature values of γ associated with each reaction. An overview of the parametrization and values used for the different reaction probabilities is given in Table 2. ECHAM-HAMMOZ and EMEP MSC-W use the same reaction probabilities or functions for many reaction, with the most important difference being the lack of ammonium nitrate aerosol in ECHAM-HAMMOZ. Lastly, to check if the surface area density is realistic, simulated S<sub>a</sub> is compared to a satellite-model-product in section 5.1.



### 3.1 N<sub>2</sub>O<sub>5</sub>

N<sub>2</sub>O<sub>5</sub> reaction probability depends on aerosol water content and aerosol composition. Therefore, several laboratory studies measured  $\gamma$  values on different aerosol types leading to the possibility to derive detailed parametrizations (Riemer et al., 2003b, 2009; Evans and Jacob, 2005; Liao and Seinfeld, 2005; Davis et al., 2008; Bertram and Thornton, 2009; Griffiths et al., 2009; Brown and Stutz, 2012). For dry sulphate aerosol, reaction probabilities range between  $10^{-4}$  and  $10^{-3}$ ; for wet aerosol  $\gamma$  ranges between  $10^{-3}$  and  $8.6 \times 10^{-2}$  depending on relative humidity. The N<sub>2</sub>O<sub>5</sub> heterogeneous reaction humidity dependence also explains the range of reaction probabilities of sea salt aerosol of  $6 \times 10^{-3}$  to  $4 \times 10^{-2}$ . On nitrate containing aerosol lower reaction probabilities were found due to nitrate effect (Wahner et al., 1998), between  $3 \times 10^{-4}$  and  $3 \times 10^{-3}$  (Chang et al. 2011b, and references therein). Moreover, N<sub>2</sub>O<sub>5</sub> can react on organic aerosol under dry conditions with low reaction probabilities in the order of  $10^{-6}$  and  $10^{-5}$  (Gross et al., 2009). This value increases to  $10^{-4}$  –  $10^{-3}$  under wet conditions, because the higher water content allows N<sub>2</sub>O<sub>5</sub> to hydrolyze (Thornton et al., 2003). Even dust aerosols can be covered by a layer of water leading to a reaction probability between  $3 \times 10^{-3}$  at 30 % and  $2 \times 10^{-2}$  at 70% relative humidity (Bauer et al., 2004). For N<sub>2</sub>O<sub>5</sub> reaction on black carbon, Sander et al. (2006) reported a wide range of reaction probabilities, between  $2 \times 10^{-2}$  –  $10^{-6}$ .

Most studies have used laboratory data to estimate  $\gamma$  values, but some have made use of ambient data. Brown et al. (2009) used aircraft measurements over Texas, and found observation-based  $\gamma$  values of ca.  $5 \times 10^{-1}$ – $6 \times 10^{-3}$ , usually substantially lower (often a factor of 10) than values calculated using laboratory-based values. Using aircraft measurements around the United Kingdom, Morgan et al. (2015) found rather high  $\gamma$  values for N<sub>2</sub>O<sub>5</sub>, from ca.  $1 \times 10^{-2}$ – $3 \times 10^{-2}$ , with strong dependencies on sulphate, and a clear suppression of  $\gamma$  due to nitrate. They concluded that including the suppressive effect of organic aerosol in the uptake parameterisation leads to significant underprediction of the  $\gamma$  values. Further, direct N<sub>2</sub>O<sub>5</sub> measurements retrieved a highly daily variation of  $\gamma_{\text{N}_2\text{O}_5}$  also explained by the nitrate effect leading to a mean value of  $5.4 \times 10^{-3}$  ranging from  $3 \cdot 10^{-5}$  to  $2.9 \cdot 10^{-2}$  (Riedel et al., 2012). In Stone et al. (2014) and Wagner et al. (2013) in situ measurements of N<sub>2</sub>O<sub>5</sub> were used to retrieve the reaction probability within the framework of a box model. In Stone et al. (2014)  $\gamma_{\text{N}_2\text{O}_5}$  is varied over a range of values between 0 and 1, and found that values of  $2 \cdot 10^{-1}$  –  $2 \cdot 10^{-2}$  agreed best with observations. Wagner et al. (2013) retrieved the reaction probability of N<sub>2</sub>O<sub>5</sub> using a box model driven by ambient wintertime observations. The reaction probability distribution ranges between  $2 \cdot 10^{-3}$  and  $1 \cdot 10^{-1}$ , displaying a maximum at  $2 \cdot 10^{-2}$ .

It is clear from the above mentioned studies that great uncertainties surround both the magnitude and the chemical dependence of  $\gamma$  values for N<sub>2</sub>O<sub>5</sub>. Even thorough evaluations such as those of Davis et al. (2008) or Chang et al. (2011a) have little consideration of important components of the aerosol such as organic matter, and even such schemes seem to be inconsistent with the aircraft-observations discussed above. For our modelling studies, we have not tried to develop or use yet another scheme, but rather to make use of the  $\gamma$  schemes already implemented in each model, with some small efforts at harmonisation to build similar reference schemes.

The equations used for EMEP MSC-W and ECHAM-HAMMOZ can be found in Table 2. Both models make extensive use of the parameterizations developed by Evans and Jacob (2005), with the largest difference being that EMEP includes ammonium nitrate (in fine particles) among the nitrate species. For N<sub>2</sub>O<sub>5</sub> the uptake coefficients for sulphate, sea salt and





organic aerosol are identical in the two models. For the reaction on dust, both models rely on Bauer et al. (2004) which was interpreted differently by Evans and Jacob (2005) and Liao and Seinfeld (2005). This small difference in the uptake coefficient formulation on dust does not lead to large differences in the resulting uptake coefficient.

- 5 EMEP MSC-W also modifies the  $\gamma$  value for secondary inorganic aerosol to account for a nitrate inhibition effect (Wahner et al., 1998; Riemer et al., 2003a). This makes use of the  $\gamma_{\text{NO}_3}$  factor presented in Davis et al. (2008) for ammonium nitrate, and merged with the sulphate factor in a manner reminiscent of Riemer et al. (2003b). First a sulphate mass fraction within the secondary inorganic aerosol is calculated (SIA),  $f_{\text{SO}_4} = m_{\text{SO}_4} / (m_{\text{SO}_4} + m_{\text{NO}_3})$ , then  $\gamma_{\text{SIA}}$  as

$$\gamma_{\text{SIA}} = f_{\text{SO}_4} \gamma_{\text{SO}_4} + (1 - f_{\text{SO}_4}) \gamma_{\text{NO}_3}. \quad (3)$$

- 10 Figure 1 illustrates the  $\gamma$  values for sulphate aerosol from Evans and Jacob (2005) as a function of relative humidity (RH) and temperature for sulphate, and the RH dependency of  $\gamma$  for nitrate from the Davis et al. (2008) formulation. The negative temperature dependence after 280K can be explained by increasing volatility with increasing temperature leading to less uptake on the aerosol. As described before, reaction probability increases with increasing water content in the aerosol due to enhanced  $\text{N}_2\text{O}_5$  hydrolysis. Even at high RH, reaction probability on nitrate containing aerosol is not as high as in sulphate aerosol.
- 15 Nevertheless, the very high  $\gamma$  values found at high RH seem questionable, because the aerosol itself becomes saturated at high RH and these small water content changes should not have such a huge impact on the heterogeneous reaction.

No further parameterization considering organic coatings is used in either EMEP MSC-W or ECHAM-HAMMOZ due to the large uncertainties in this effect (e.g. Brown et al., 2009; Morgan et al., 2015), and the fact that ambient OM and its thermodynamic properties are so poorly understood (Hallquist et al., 2009). Further, sensitivity runs done with ECHAM-HAMMOZ have shown minor global impact of organic coatings (Stadtler, 2015).

### 5 3.2 $\text{NO}_3$

Hydrolysis of the nitrate radical  $\text{NO}_3$  happens on various aerosol types depending on the water content.  $\text{NO}_3$  heterogeneous reaction produces  $\text{HNO}_3$  and OH in the aqueous particle phase and can be counted as a  $\text{NO}_x$  sink (Rudich et al., 1998). Several laboratory studies shown  $\gamma$  ranging between  $10^{-4}$  and  $10^{-3}$  (Rudich et al., 1996; Moise et al., 2002). Jacob (2000) recommended to use  $\gamma = 10^{-3}$  for atmospheric chemistry model simulations, and this value was adopted for EMEP and

- 10 ECHAM-HAMMOZ.

### 3.3 $\text{NO}_2$

$\text{NO}_2$  heterogeneous reaction leads to the production of  $\text{HNO}_3$  and HONO. Especially in humid environments, the heterogeneous reaction may account for up to 95% of HONO production (Goodman et al., 1999). During nighttime HONO can accumulate in the atmosphere and therefore be an efficient OH radical source during the morning when sun rise starts photolysis (ibid). Estimates of  $\gamma$  for  $\text{NO}_2$  vary widely, however, with several laboratory studies giving a range between  $10^{-8}$  and  $10^{-3}$

- 15

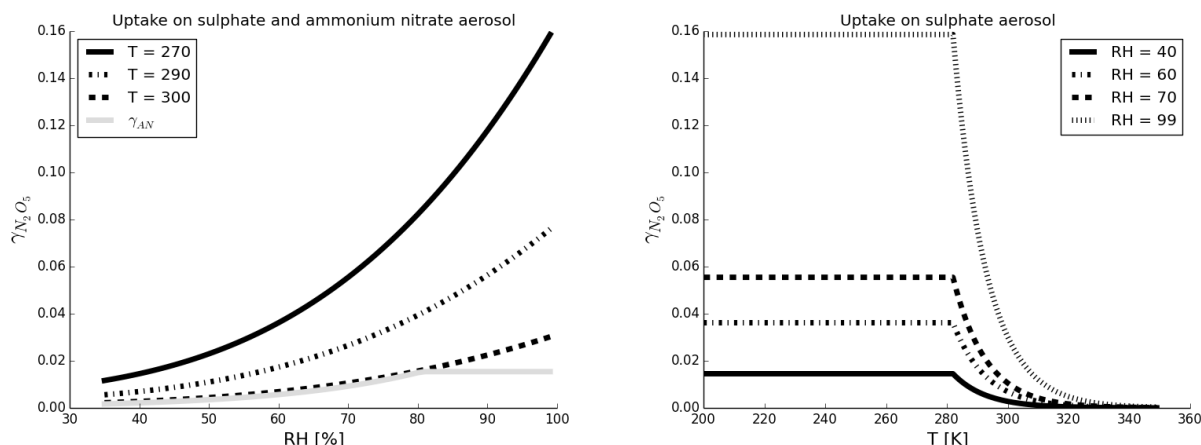


**Figure 1.** Upper plot:  $N_2O_5$  reaction probability dependence on relative humidity for sulphate (black) and nitrate (grey) aerosol. For sulfate aerosol three temperatures are shown. Lower plot:  $N_2O_5$  reaction probability temperature dependence on sulphate aerosol for four relative humidity. Parameterizations from Evans and Jacob (2005) and Davis et al. (2008), see text.

(Harrison and Collins, 1998; Kleffmann et al., 1998; Arens et al., 2001; Underwood et al., 2001). Jacob (2000) recommended  $\gamma = 10^{-4}$  and this value is used for this study.

### 3.4 $HNO_3$

Nitric acid reacts on sea salt and dust aerosol surfaces, producing nitrate which stays in the aerosol phase (Davies and Cox, 1998; Hodzic et al., 2006). Experimentally derived  $\gamma$  values for  $HNO_3$  on sea salt range between  $10^{-4}$  and  $10^{-2}$  (Davies and Cox 1998, and references therein). A relative humidity dependent uptake coefficient was proposed in Hauglustaine et al. (2014) increasing  $\gamma$  from  $10^{-3}$  and  $10^{-1}$  to cover low and high relative humidity. No such relative humidity dependence was used in this study, because for the conditions in the marine boundary layer, the value of  $10^{-2}$  fits well and is used here.

Heterogeneous reaction of  $HNO_3$  on dust was studied on different types of minerals, atmospheric dust types and for a range of relative humidities giving  $\gamma$  in the range of  $10^{-6}$  and  $10^{-1}$  (Hanisch and Crowley, 2001; Usher et al., 2003; Liu et al., 2008; Hauglustaine et al., 2014). Although in Fairlie et al. (2010) a relative humidity dependence of varying  $\gamma$  between  $10^{-5}$  and  $10^{-3}$  is described, the value is used here is based on Hodzic et al. (2006), who tested  $\gamma$  values between  $10^{-6}$  and 0.3, deriving 0.1 as the best  $\gamma$  value minimizing the model error compared to observations. Compared to the other referenced studies, this is an upper limit.

### 3.5 $O_3$

Studies of the heterogeneous reaction of ozone on dust give a wide range for possible reaction probabilities, from  $10^{-10}$  to  $10^{-4}$  (Reus et al., 2000; Usher et al., 2003; Mogili et al., 2006; George et al., 2015). Reus et al. (2000) gives  $10^{-4}$  as an upper





limit for this reaction probability, but George et al. (2015) suggests a more conservative upper limit value of  $10^{-5}$ . Nevertheless, Nicolas et al. (2009) conclude that a reaction probability of  $10^{-6}$  is a realistic number in terms of atmospheric environmental conditions, and this value was adopted here.

### 3.6 HO<sub>2</sub>

- 10 HO<sub>2</sub> reaction probability is highly variable and strongly depends on transition metal ions contained in the aerosol (Tilgner et al., 2005; Mao et al., 2013; George et al., 2013; Huijnen et al., 2014). Furthermore, this reaction can also take place on cloud droplets. Estimates for  $\gamma$  range between 0.02 and 1 (Jacob, 2000; Remorov et al., 2002; Thornton and Abbatt, 2005; Taketani et al., 2008; George et al., 2013; Mao et al., 2013). Whalley et al. (2015) measured HO<sub>2</sub> in clouds and found a decrease in HO<sub>2</sub> concentrations up to 90%. Depending on the compounds in the particle aqueous phase heterogeneous reaction of HO<sub>2</sub> produces
- 15 either H<sub>2</sub>O<sub>2</sub> or H<sub>2</sub>O. Consequently, this heterogeneous reaction can be a terminal radical sink or not (Mao et al., 2013; Whalley et al., 2015). Here we do not account for a terminal sink, but let the heterogeneous reaction of HO<sub>2</sub> produce H<sub>2</sub>O<sub>2</sub> and use the  $\gamma$  recommended by Jacob (2000) of 0.2.

## 4 Setup of sensitivity runs

- To test the six heterogeneous reactions (see Table 1), six sensitivity runs were designed and performed with both models. For
- 20 EMEP MSC-W a spin up of six months and for ECHAM-HAMMOZ one of twelve months is used. Afterwards the results for the whole year 2012 are evaluated. The reference run REF contains all heterogeneous reactions with the parameterizations given in Table 2. Each sensitivity run is done with five out of six heterogeneous reactions; the names of the runs show which compound does not undergo heterogeneous reaction. For example, in the noN<sub>2</sub>O<sub>5</sub> run, only N<sub>2</sub>O<sub>5</sub> heterogeneous reaction is turned off. An overview of the simulation is given in Table 3.



**Table 1.** Heterogeneous reactions in the EMEP MSC-W and ECHAM-HAMMOZ models. The second column specifies the aerosol type on which the reaction proceeds in the models: SS: seasalt, DU: dust, PM: particulate matter

No.	Reaction	Aerosol type	Notes
R1	$\text{N}_2\text{O}_5 \longrightarrow 2\text{HNO}_3$	PM	1
R2	$\text{NO}_3 \longrightarrow \text{HNO}_3$	PM	2
R3	$\text{NO}_2 \longrightarrow \frac{1}{2}\text{HNO}_3 + \frac{1}{2}\text{HONO}$	PM	2
R4	$\text{HNO}_3 \longrightarrow \text{NO}_3^-$	SS, DU	2,3
R5	$\text{HO}_2 \longrightarrow \frac{1}{2}\text{H}_2\text{O}_2$	PM	2
R6	$\text{O}_3 \longrightarrow \text{HO}_2$	DU	

<sup>1</sup> Just for RH>40% in EMEP.

<sup>2</sup> Just on wet aerosol in ECHAM-HAMMOZ.

<sup>3</sup> Just on coarse mode dust and sea-salt in EMEP, using  $S_{\text{SS}}$  and/or  $S_{\text{du}}$ , see Sect. 2.1.



**Table 2.** Reaction probabilities for the different species. Unless explicitly labelled (in parentheses after the equation), both models use the same formulation. Here, RH denotes relative humidity in range,  $RH \in (0, 100)$ , and fRH denotes fractional relative humidity in range,  $fRH \in (0, 1)$ .

Specie	$\gamma$	Reference
$N_2O_5$	$\gamma_{SS} = \begin{cases} 0.005, RH \leq 62 \% \\ 0.03, RH \geq 62 \% \end{cases}$	EVA05
	$\gamma_{SU} = \alpha \cdot 10^{-\beta}$	EVA05
	$\alpha = 2.79 \cdot 10^{-4} fRH + 1.3 \cdot 10^{-4} fRH - 3.43 \cdot 10^{-6} fRH^2 + 7.52 \cdot 10^{-8} fRH^3$	
	$\beta = \begin{cases} 4 \cdot 10^{-2} (T - 294), T > 282 \text{ K} \\ -0.48, T \leq 282 \text{ K} \end{cases}$	
	$\gamma_{DU} = 0.01$ (EMEP)	EVA05
	$\gamma_{DU} = 4.25 \cdot 10^{-4} RH - 9.75 \cdot 10^{-3} (30\% \leq RH \leq 70\%)$ (ECHAM)	LIA05
	$\gamma_{OC} = \begin{cases} 0.03, RH > 57\% \\ 5.2 \cdot 10^{-2}, RH \leq 57\% \end{cases}$	
	$\gamma_{BC} = 0.005$	EVA05
	$\gamma_{AN} = \min(0.0154, 1/(1 + \exp(8.10774 - 0.04902 \cdot RH)))$ (EMEP)	DAV08
$NO_3$	$\gamma = 0.001$	JAC00
$NO_2$	$\gamma = 10^{-4}$	JAC00
$HNO_3$	$\gamma_{SS} = 0.01$	DAV98
	$\gamma_{DU} = 0.1$	HOD06
$HO_2$	$\gamma = 0.2$	JAC00
$O_3$	$\gamma_{DU} = 10^{-6}$	NIC09

The subscripts refer to the aerosol compounds as given in Table 1, plus OC:Organic carbon/Organic matter, SU: Sulphate;BC black carbon.

Refs: DAV98 Davies and Cox (1998), DAV08 Davis et al. (2008), EVA05 Evans and Jacob (2005), JAC00 Jacob (2000), LIA05 Liao and Seinfeld (2005), THO08 Thornton et al. (2008), HOD06 Hodzic et al. (2006), NIC09 Nicolas et al. (2009)



**Table 3.** Overview of sensitivity runs.

Run	Description
REF	All heterogeneous reactions
noN2O5	All except $\text{N}_2\text{O}_5$ reaction
noNO3	All except $\text{NO}_3$ reaction
noNO2	All except $\text{NO}_2$ reaction
noHNO3	All except $\text{HNO}_3$ reaction
noHO2	All except $\text{HO}_2$ reaction
noO3	All except $\text{O}_3$ reaction



## 25 5 Results and Discussion

### 5.1 Surface area density

Aerosols consist of a variety of compounds in the gas, liquid or solid phase, and the shapes of aerosols vary greatly (Pöschl, 2005). Large scale models can not explicitly treat the morphology of aerosols. In EMEP MSC-W and ECHAM-HAMMOZ distribution functions and median radii are used to simulate the aerosol population. Based on this approach surface area density  
 30  $S_a$  is calculated considering the aerosol distribution, the median radius and assuming spherical particles. This assumption is good for liquid aerosols behaving as small water droplets. For dry particles this assumption can lead to an underestimation of  $S_a$  due to folded or porous structures (Buseck and Posfai, 1999).

In van Donkelaar et al. (2015) satellite retrievals and the GEOS-Chem chemical transport model are used to derive global surface  $PM_{2.5}$  estimates with a resolution of  $10\text{ km} \times 10\text{ km}$  in the time period between 1998 and 2012. The physical relation between AOD and surface area is described in the supplementary material of van Donkelaar et al. (2015).

Figure 2 shows the estimated  $PM_{2.5}$  surface area by van Donkelaar et al. (2015) and the modeled surface area density  
 5  $S_a$  from EMEP MSC-W and ECHAM-HAMMOZ as annual mean 2012 over land. Although these data-sets are not strictly comparable, since the van Donkelaar et al. 2015 estimate in itself relies partly on various assumptions of a third chemical transport model, GEOS-Chem (*ibid*), the general patterns of the models agree well with the surface area density estimation. Both models capture the east west gradient in  $S_a$  over North America even if the total  $S_a$  value is comparably lower in both models. Similarly, Europe in the satellite GEOS-Chem product has slightly higher  $S_a$  values than the models produce. In  
 10 contrast, the  $S_a$  values over India are captured very well, and the peak values in East Asia are also produced by both models, while ECHAM-HAMMOZ simulates highest  $S_a$  values among the three data sets in East Asia. An overestimation of both models compared to satellite GEOS-Chem happens over North Africa. In South America EMEP MSC-W performs better than ECHAM-HAMMOZ due to larger contributions from secondary organic aerosol (SOA) formation. EMEP uses a more complex SOA scheme (Bergström et al., 2012; Simpson et al., 2012) which allows for oxidation ('aging') of semivolatile  
 15 organic vapours. In ECHAM-HAMMOZ an adjusted amount of organic material covering also SOA is emitted, but the amount does not close the gap leading to a lower  $S_a$  compared to EMEP MSC-W and satellite GEOS-Chem.

### 5.2 Impacts of sensitivity tests

To evaluate the impact of our heterogeneous reactions, the six sensitivity runs were compared to the reference run containing all heterogeneous reactions. By turning off one heterogeneous reaction in each sensitivity run, the impact of each reaction can  
 20 be estimated. Table 4 and 5 show the differences between the sensitivity runs and the reference run for EMEP MSC-W and ECHAM-HAMMOZ, as averaged over regions of North America (NA), Europe (EUR), East Asia (EA) and South Asia (SA) defined like in Fiore et al. 2009. The main focus of this evaluation lies on the effect of the heterogeneous reactions on ozone mixing ratios.

For the reference runs, EMEP MSC-W and ECHAM-HAMMOZ simulate very similar values for ozone, ECHAM-HAMMOZ  
 25 giving somewhat lower mixing ratios. Also  $NO_x$  values are similar in Asia, but differ 50 % to 100 % in North America and



**Table 4.** Impacts of gas-aerosol reactions on regional average mixing ratios of O<sub>3</sub> and key NO<sub>y</sub> compounds: EMEP model.

Region	Run	O <sub>3</sub> (ppb)	NO <sub>x</sub> (ppb)	NO <sub>y</sub> (ppb)	HNO <sub>3</sub> (ppb)	PAN (ppb)	N <sub>2</sub> O <sub>5</sub> (ppt)	NO <sub>3</sub> (ppt)
NA	REF	39.830	0.863	1.824	0.213	0.513	12.27	5.01
NA	noN2O5	-3.788	-0.122	-0.210	0.012	-0.086	-34.02	-4.13
NA	noHO2	-0.061	0.010	0.001	-0.002	-0.007	0.25	0.50
NA	noHNO3	-0.121	0.0	0.041	-0.038	-0.0	0.01	-0.01
NA	noNO2	-0.190	-0.018	-0.014	0.001	-0.001	-0.47	-0.11
NA	noNO3	-0.084	-0.0	-0.001	0.0	-0.001	-0.10	-0.17
NA	noO3	-0.012	0.0	0.0	-0.0	-0.0	-0.00	-0.00
EUR	REF	40.607	1.023	2.432	0.256	0.508	16.43	7.33
EUR	noN2O5	-4.539	-0.292	-0.360	0.029	-0.104	-86.73	-8.06
EUR	noHO2	-0.300	0.027	0.004	-0.002	-0.020	0.64	0.94
EUR	noHNO3	-0.273	0.0	0.153	-0.149	-0.0	0.00	-0.20
EUR	noNO2	-0.160	-0.046	-0.028	0.001	0.004	-0.96	-0.30
EUR	noNO3	-0.163	-0.001	-0.003	0.0	-0.001	-0.38	-0.80
EUR	noO3	-0.051	0.0	0.0	-0.0	0.0	-0.00	-0.01
EA	REF	43.441	2.271	4.657	0.548	0.842	28.29	6.29
EA	noN2O5	-5.637	-0.481	-0.591	0.073	-0.180	-123.3	-10.17
EA	noHO2	-0.815	0.080	0.006	-0.011	-0.063	-0.04	0.48
EA	noHNO3	-0.114	0.002	0.083	-0.073	-0.0	0.02	0.00
EA	noNO2	0.354	-0.677	-0.421	0.060	0.067	-3.96	-0.30
EA	noNO3	-0.096	-0.0	-0.001	0.0	-0.001	-0.39	-0.21
EA	noO3	-0.017	0.0	0.0	-0.0	-0.0	-0.00	-0.00
SA	REF	47.010	1.140	2.932	0.421	0.313	24.38	12.86
SA	noN2O5	-3.799	-0.146	-0.120	0.007	-0.059	-40.12	-9.36
SA	noHO2	-0.273	0.033	0.010	-0.004	-0.016	1.22	1.59
SA	noHNO3	-0.680	-0.0	0.236	-0.260	-0.001	-0.23	-0.49
SA	noNO2	-0.357	-0.048	-0.036	0.001	-0.003	-2.56	-0.70
SA	noNO3	-0.469	-0.003	-0.008	-0.0	-0.002	-1.33	-1.44
SA	noO3	-0.043	0.0	-0.0	-0.0	-0.0	-0.00	-0.01

The first column refers to the region over which the annual mean is spatially averaged, and the second column refers to the corresponding run. Values shown for the reference run are total mixing ratios in ppbv. For all sensitivity runs only field averaged differences in ppbv are shown. Since the the sensitivity runs were subtracted from the reference run, positive values mean higher mixing ratios in the reference run than in the sensitivity runs and vice versa. Regions are defined as follows: NA (15°N–55°N; 60°W–125°W), EU (25°N–65°N; 10°W–50°E), EA (15°N–50°N; 95°E–160°E), and SA (5°N–35°N; 50°E–95°E).





**Table 5.** Same as table 4, but for ECHAM-HAMMOZ.

Region	Run	O <sub>3</sub> (ppb)	NO <sub>x</sub> (ppb)	NO <sub>y</sub> (ppb)	HNO <sub>3</sub> (ppb)	PAN (ppb)	N <sub>2</sub> O <sub>5</sub> (ppt)	NO <sub>3</sub> (ppt)
NA	REF	38.936	1.293	1.591	0.146	0.135	14.85	2.71
NA	noN2O5	-2.163	-0.086	-0.125	-0.012	-0.011	-13.99	-1.52
NA	noHO2	-0.089	0.014	0.009	-0.003	-0.002	0.04	0.07
NA	noHNO3	-2.233	0.01	-0.18	-0.186	-0.003	-0.91	-0.29
NA	noNO2	-0.186	-0.027	-0.025	0.001	0.001	-0.46	-0.06
NA	noNO3	-0.039	0.0	0.001	0.0	0.0	-0.05	-0.04
NA	noO3	-0.071	0.001	0.001	-0.0	0.0	-0.05	-0.01
EUR	REF	39.566	2.034	2.376	0.154	0.161	21.51	4.7
EUR	noN2O5	-2.815	-0.215	-0.297	-0.019	-0.022	-38.0	-2.88
EUR	noHO2	-0.385	0.036	0.023	-0.005	-0.009	0.16	0.17
EUR	noHNO3	-2.163	0.019	-0.335	-0.349	-0.003	-1.37	-0.68
EUR	noNO2	-0.113	-0.118	-0.106	0.005	0.008	-1.16	-0.15
EUR	noNO3	-0.052	-0.0	-0.001	-0.0	0.0	-0.13	-0.13
EUR	noO3	-0.09	0.003	0.003	0.0	0.0	-0.07	-0.02
EA	REF	38.505	2.101	2.541	0.17	0.258	10.05	2.64
EA	noN2O5	-3.333	-0.24	-0.338	-0.026	-0.038	-31.27	-3.02
EA	noHO2	-0.816	0.098	0.054	-0.009	-0.034	-0.14	0.05
EA	noHNO3	-1.852	0.013	-0.242	-0.252	-0.003	-0.52	-0.24
EA	noNO2	0.062	-0.606	-0.542	0.013	0.053	-0.97	-0.12
EA	noNO3	-0.02	-0.001	-0.001	-0.0	0.001	-0.04	-0.05
EA	noO3	-0.053	-0.001	-0.0	-0.0	0.0	-0.02	-0.0
SA	REF	44.255	1.29	1.535	0.099	0.125	15.5	6.15
SA	noN2O5	-2.219	-0.083	-0.13	-0.013	-0.017	-14.85	-2.18
SA	noHO2	-0.287	0.036	0.024	-0.005	-0.007	0.1	0.22
SA	noHNO3	-3.453	0.009	-0.604	-0.606	-0.005	-1.27	-1.06
SA	noNO2	-0.33	-0.046	-0.047	0.001	0.0	-1.25	-0.3
SA	noNO3	-0.115	0.001	-0.001	-0.0	-0.0	-0.26	-0.21
SA	noO3	-0.077	-0.0	-0.001	-0.0	-0.0	-0.04	-0.02

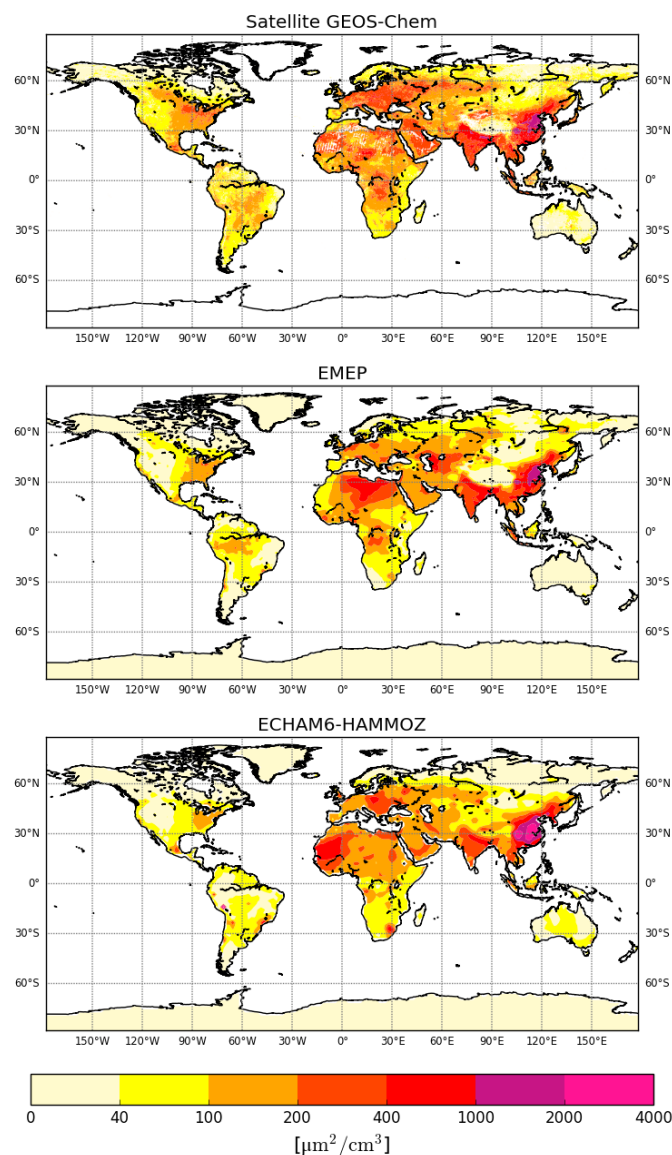


**Figure 2.** Satellite estimated (top) and simulated surface area densities by EMEP (middle) and ECHAM-HAMMOZ (bottom). The Satellite data is an average value for the time period 2010 - 2012, from van Donkelaar et al. (2015). The model data is for 2012.



Europe. In terms of other reactive nitrogen species, EMEP MSC-W has overall higher  $\text{NO}_y$  levels and especially PAN. This difference in  $\text{NO}_y$  availability is expected given the impact of EMEP's  $\text{NH}_3$  emissions in the formation of ammonium nitrate, thus extending the lifetime of reactive nitrogen species.

Tables 4–5 clearly show reductions in  $\text{O}_3$  from all the sensitivity runs, except for the sensitivity run without heterogeneous  $\text{NO}_2$  reaction in East Asia. In this region the special case of ozone titration (Wild and Akimoto, 2001) leads to an ozone loss due to  $\text{NO}_2$  instead of production: lowering  $\text{NO}_2$  in this region of very high  $\text{NO}_x$  regions means reducing a loss process. Even if the models agree on the direction of the impact of heterogeneous reaction on  $\text{O}_3$ , they do not agree on the strength of the reactions.

For both models the  $\text{N}_2\text{O}_5$  reactions have generally (ECHAM-HAMMOZ) or always (EMEP) the biggest effect on  $\text{O}_3$ , with changes of ca. 2–6 ppb. The EMEP model shows a consistently larger response in all regions. Some other heterogeneous reactions (especially  $\text{NO}_2$ ,  $\text{HO}_2$  and  $\text{HNO}_3$ ) gain some significance in highly polluted areas where aerosol surface areas are high, but the two models show quite different response though in their response to these other gas-aerosol reactions. The EMEP model actually shows rather small impacts of all reactions except  $\text{N}_2\text{O}_5$ , except in East and South Asia where some impacts can approach 10–20% of that of  $\text{N}_2\text{O}_5$ . ECHAM-HAMMOZ, on the other hand, shows quite marked responses to especially the  $\text{HNO}_3$  reactions, but also the  $\text{HO}_2$  reactions.

The strong response of  $\text{O}_3$  in ECHAM-HAMMOZ to the  $\text{HNO}_3$  reaction compared to EMEP seems to be the result of a number of factors. The simplest is that EMEP allows this reaction only on coarse aerosol, and so has a smaller surface area for this reaction, especially on dust. Another explanation is that the model sensitivities to  $\text{NO}_x$  changes may be different, possibly caused by chemical differences or the different horizontal resolutions of the models. Ozone chemistry (and even the switch from production to loss) can be very sensitive to  $\text{NO}_x$  concentration levels, especially in unpolluted areas (Crutzen et al., 1999; Sillman et al., 1990).  $\text{NO}_x$  plumes from ships or power plants emitted into large model grid cells might well produce more  $\text{O}_3$  in one model than the other, leading to different sensitivities to  $\text{NO}_x$  emissions (von Glasow et al., 2003; Vinken et al., 2011). The EMEP model has in fact a pseudo-species ‘SHIPNO $_x$ ’ by which 50% of  $\text{NO}_x$  from ship plumes are given a pathway to  $\text{HNO}_3$  production, skipping the intermediate  $\text{NO}_2$  production associated with overestimating  $\text{O}_3$  production from NO in pristine environments (Simpson et al., 2015). A further factor is the lack of nitrate aerosol in ECHAM-HAMMOZ. In the EMEP model  $\text{HNO}_3$  can take part in ammonium nitrate aerosol (AN) formation, thus extending the lifetime of  $\text{NO}_y$ . Due to the AN, some  $\text{HNO}_3$  can be recycled back into the atmosphere stabilizing the  $\text{HNO}_3$  and  $\text{NO}_3$  mixing ratios.

Table 5 shows that for ECHAM-HAMMOZ omitting the  $\text{HNO}_3$  reaction on dust and sea salt aerosol increases  $\text{NO}_x$  by ca. 10–20 ppt, whereas in EMEP the change is tiny. The impact in ECHAM-HAMMOZ can be found over the whole globe, but especially over the oceans, where  $\text{NO}_x$  is low, but still much higher than  $\text{NO}_z$ . Changes in  $\text{NO}_z$  are far higher in ECHAM-HAMMOZ than in EMEP. Even if heterogeneous  $\text{HNO}_3$  loss does not hugely impact  $\text{NO}_x$ , a small  $\text{NO}_x$  increase, even if really small, is ubiquitous and shifts the equilibrium between ozone production and loss towards more production, reaching a higher steady state  $\text{O}_3$  concentration. Also, this reaction has a significant effect on  $\text{NO}_3$ , reducing it in the northern oceans by about 10 % (not shown).  $\text{NO}_3$  rapidly photolyses, and resulting  $\text{NO}_2$  likewise, so has a high ozone-formation potential. Reducing  $\text{HNO}_3$  and therefore  $\text{NO}_3$  drastically by the surface reaction in this highly sensitive region leads to a nonlinear response of the model



changing the gross ozone production in ECHAM-HAMMOZ by 350 Tg, which is a reduction of 7 %. This leads to a global more or less uniformly distributed difference of 1 - 4 ppbv in ozone mixing ratios.

Analyzing all the possible differences in these two different models is beyond of the scope of this study, but it may well be that  
 30 ECHAM-HAMMOZ overestimates the impact of  $\text{HNO}_3$  due to missing nitrate aerosol formation and EMEP underestimates the impact, due to the use of only coarse sea salt and dust aerosol for the  $\text{HNO}_3$  and  $\text{HO}_2$  reactions.

As the  $\text{N}_2\text{O}_5$  reactions have the greatest impact on tracer concentrations among our sensitivity tests, the spatial and temporal differences between the reference run and the sensitivity run noN2O5 have been investigated in more detail. Figs. 3 and 4 show the difference between the mixing ratios of  $\text{O}_3$  and  $\text{NO}_x$  in the reference run and in the sensitivity run without the  $\text{N}_2\text{O}_5$  reactions. Both models show the largest changes in regions where high aerosol loadings and high  $\text{NO}_x$  emissions can be found, such as Northeast America, Europe, South and East Asia.

Converting  $\text{N}_2\text{O}_5$  to  $\text{HNO}_3$  on aerosol surfaces introduces an additional sink for  $\text{NO}_x$ , because  $\text{HNO}_3$  is rapidly (in EMEP  
 5 MSC-W) or immediately (in ECHAM-HAMMOZ) lost via dry, wet deposition and reactive uptake on aerosols after it is produced. Therefore,  $\text{NO}_x$  mixing ratios are lowered in the reference run REF compared to the simulation without the heterogeneous reaction noN2O5, as can be seen in Figure 4.

For ozone, the differences propagate through the whole northern hemisphere due to the longer lifetime of  $\text{O}_3$  compared to  $\text{NO}_x$  (Fig. 3). Again both models simulate similar patterns with regard to the spatial distribution of changes due to  $\text{N}_2\text{O}_5$ . As  
 10 described before, EMEP MSC-W shows a bigger impact on  $\text{O}_3$  concentrations than ECHAM-HAMMOZ because of  $\text{O}_3$  is already lowered due to the direct heterogeneous loss of  $\text{HNO}_3$ .

Especially for East Asia the impact of heterogeneous reactions cannot be neglected. High nitrate loadings in ammonium poor regions verify the importance shown by the models (Pathak et al., 2008). In the southern hemisphere,  $\text{N}_2\text{O}_5$  and the other heterogeneous reactions evaluated in this study have much smaller impacts on ozone and  $\text{NO}_x$  than seen in the northern  
 15 hemisphere (Figures 3, 4).

To explore the seasonal impact of  $\text{N}_2\text{O}_5$  reactions, Fig. 5 shows monthly values for tracer mixing ratios and surface area density from both models for the different northern hemispheric regions. In general, the models produce comparable seasonal cycles for the gas tracers and surface area density. Strongest seasonal cycles are found in the noN2O5 run and in ozone for both runs. In the noN2O5 run,  $\text{N}_2\text{O}_5$  builds up during winter time, because it is thermally unstable and photolabile. Including  
 20 the heterogeneous uptake leads to a strong  $\text{N}_2\text{O}_5$  reduction in both models, yielding a flat seasonal curve. The loss of  $\text{N}_2\text{O}_5$  leads to a decrease in  $\text{NO}_2$ ,  $\text{NO}_3$  and PAN. Here models slightly differ. EMEP displays a stronger reduction in  $\text{NO}_3$  and PAN, since it has in both runs higher mixing ratios compared to ECHAM-HAMMOZ. Removing  $\text{NO}_2$  from the system leads in both models to a reduction of ozone. Although, the impact of  $\text{N}_2\text{O}_5$  heterogeneous reaction on  $\text{NO}_2$  is higher in winter and lowest during summer, the greatest change in  $\text{O}_3$  can be found during spring. This can be explained by the availability of  $\text{N}_2\text{O}_5$  and  
 25 ozone production strength. As stated before,  $\text{N}_2\text{O}_5$  is formed during night time, therefore less sun is favorable. In contrast, to form ozone light is needed. Still high  $\text{N}_2\text{O}_5$  concentrations, enough surface area and a sufficiently high ozone production can be found during spring, leading to the biggest change in  $\text{O}_3$  production during this season. During winter, nights are longer and the sun is less active, therefore also heterogeneous chemistry is efficient, but less ozone production reduction occurs.

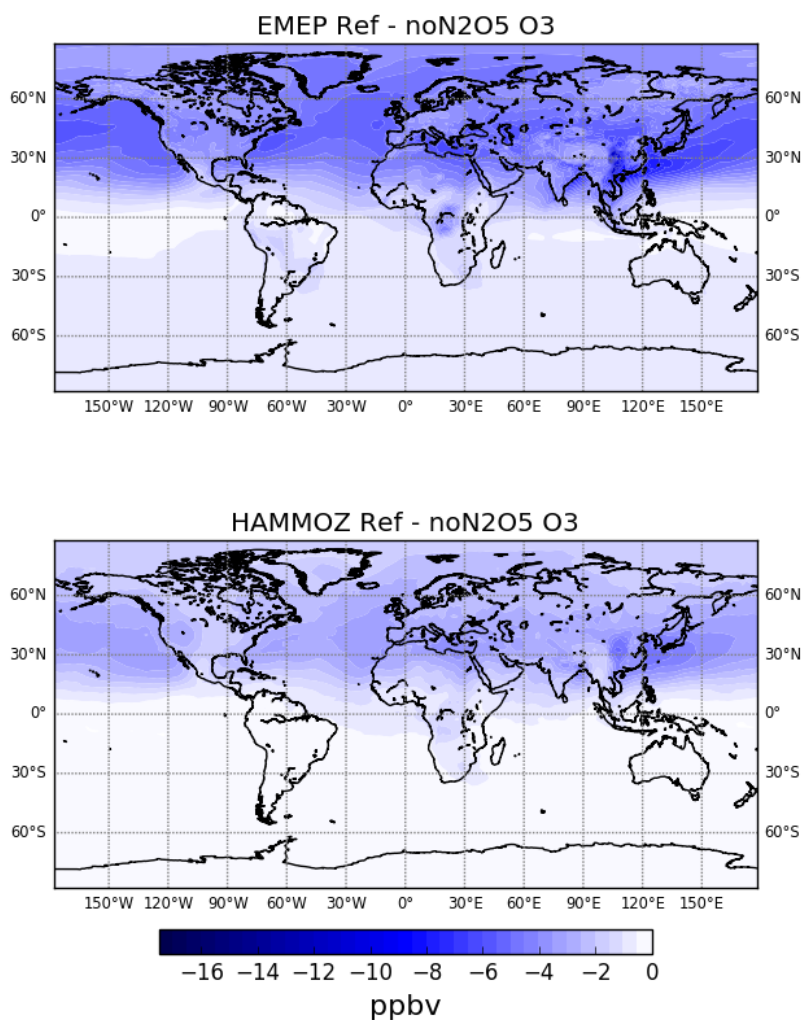


**Figure 3.** Differences in annual mean ozone mixing ratio between the reference run REF and the sensitivity run noN2O5 for 2012. Since the sensitivity run was subtracted from the reference run, negative values show higher values in noN2O5 than in REF.

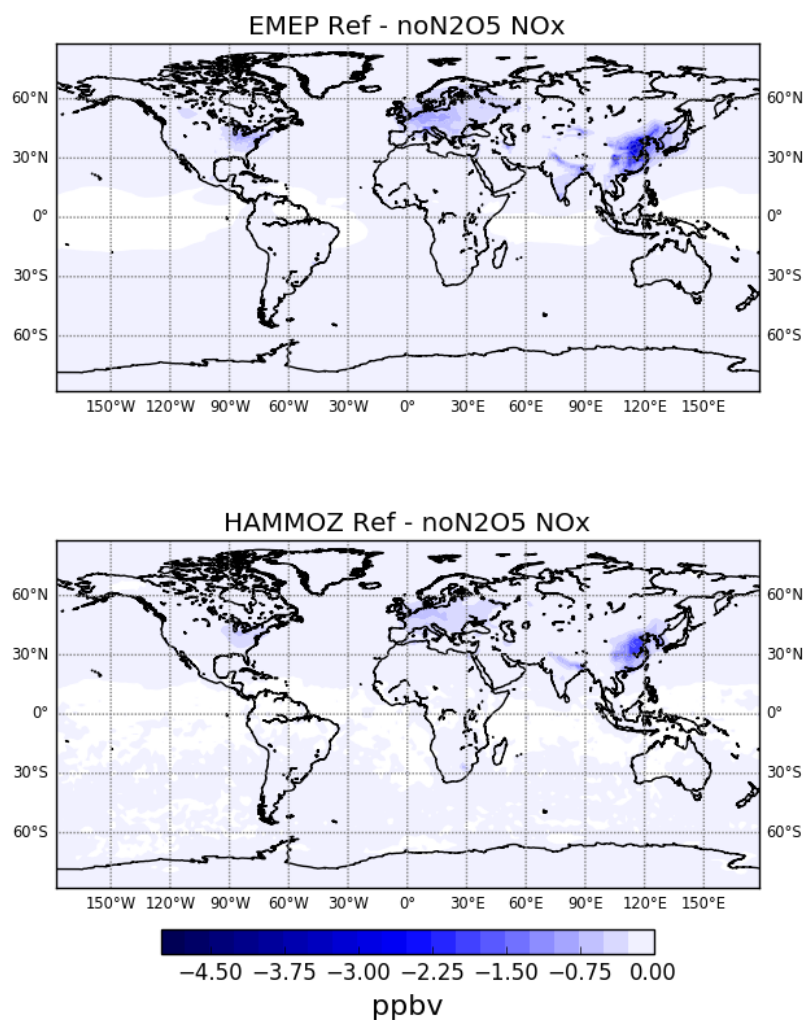


**Figure 4.** Differences in annual mean  $\text{NO}_x$  mixing ratio between the reference run REF and the sensitivity run noN2O5 for 2012. Since the sensitivity run was subtracted from the reference run, negative values show higher values in noN2O5 than in REF.



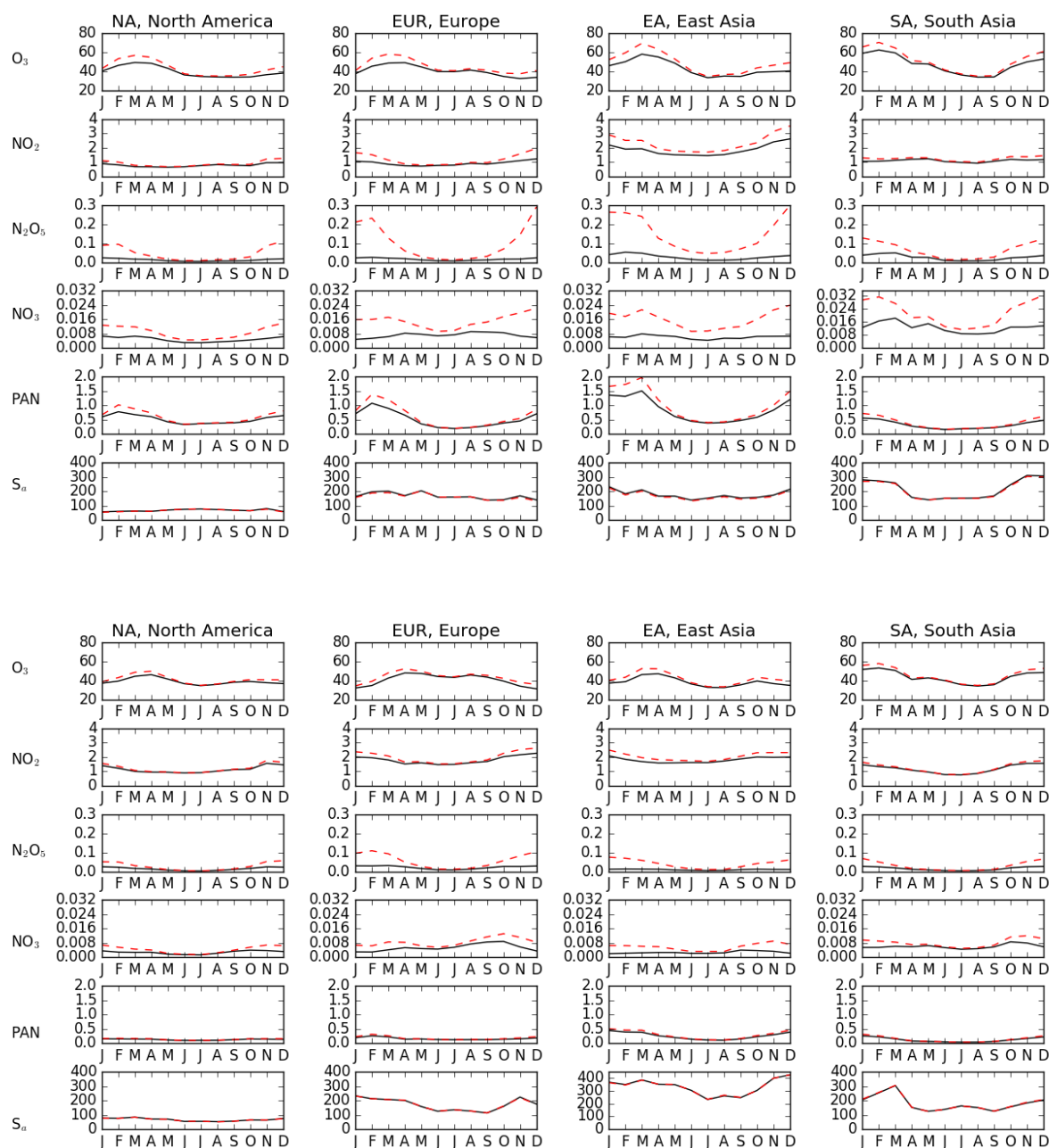


**Figure 5.** Changes in  $\text{O}_3$ ,  $\text{NO}_2$ ,  $\text{N}_2\text{O}_5$ ,  $\text{NO}_3$ , PAN and  $S_a$  for the base-case (solid black line) and noN2O5 case (dashed red line) for EMEP (top) and ECHAM-HAMMOZ (bottom). Plots show monthly gas phase mixing ratios in ppbv and surface area density in  $\mu\text{m}^2\text{cm}^{-3}$  for different regions as defined above.



### 5.3 Comparison with observations

- 30 Surface observations from 20 sites of the GAW and TOAR networks (Global Atmospheric Watch, Schultz et al. 2015, 2017), with stations distributed over the world, were used to evaluate ozone concentrations in the reference and  $\text{N}_2\text{O}_5$  sensitivity runs of both models. The GAW data set consists of many sites in North America and Europe, but unfortunately few in Asia (e.g. none in China for 2012). Still, sites exist in Japan and these should provide a good indication of ozone formation downwind of the mainland. Mountain sites were excluded from this comparison in order to avoid problems with the interpretation of which
- 5 model level is most appropriate for comparison. Trinidad Head on the west coast of USA and Mace Head on the west coast of Ireland are also good background stations which capture trends in hemispheric air masses arriving from the Pacific and Atlantic respectively (Parrish et al., 2009, 2014). To capture the seasonal dependence of  $\text{N}_2\text{O}_5$  uptake on aerosol, daily maximum ozone values were compared with the corresponding interpolated model data. Since the stations were selected to be relatively remote and low-elevation, ground stations the comparison with the coarse grids of the models might be representative.
- 10 Six out of the twenty stations are shown in Figs. 6, 7 and 8. Both models generally capture the seasonal variation well, fine structures and fluctuations are often reproduced, but not equally well by both models and depending on the station. For example in Tsukuba, Japan both models simulate the increasing variability during summer time, nevertheless maximum concentrations are still underestimated. EMEP calculates higher peak values, than ECHAM-HAMMOZ, in contrast in Waldhof, Germany, ECHAM-HAMMOZ simulates higher peak values, partially overestimating them compared to the observations.
- 15 A closer look at the dashed line compared to the solid line reveals the seasonal highest impact of  $\text{N}_2\text{O}_5$  during spring time. The high impact in spring pattern can be found in both model simulations, but is stronger in EMEP, since ECHAM-HAMMOZ includes the year through ozone reduction due to direct  $\text{HNO}_3$  loss explained in the previous section 5.2. For example in Mace Head, Ireland the springtime ozone formation is clearly decreased by  $\text{N}_2\text{O}_5$  reaction, while during summer the impact is marginal and increases again during winter. Both models start with a spin-up from the reference run, therefore the winter
- 20 impact can not be seen in January. If the models would run for another month, this would show too, indicated by the gap between reference run and no $\text{N}_2\text{O}_5$  sensitivity run at the very end of the year.

Concluding, the impact of  $\text{N}_2\text{O}_5$  heterogeneous reactions on chemical ozone production leads to a better agreement of EMEP and ECHAM-HAMMOZ and daily maximum ozone station observations in remote stations. Both models show improvements due to prior slight ozone overestimation. Heterogeneous chemistry removing ozone in models which tend to overestimate it,

25 logically improve the model. This improvements could also be done introducing other nitrogen species loss process to reduce ozone production, less  $\text{NO}_x$  emissions or dynamically inhibiting downward transport of stratospheric ozone. Especially the stratospheric ozone intrusion is assumed to strongly happen during spring time, which would cause the same pattern as we see here in Figures 6, 7 and 8.

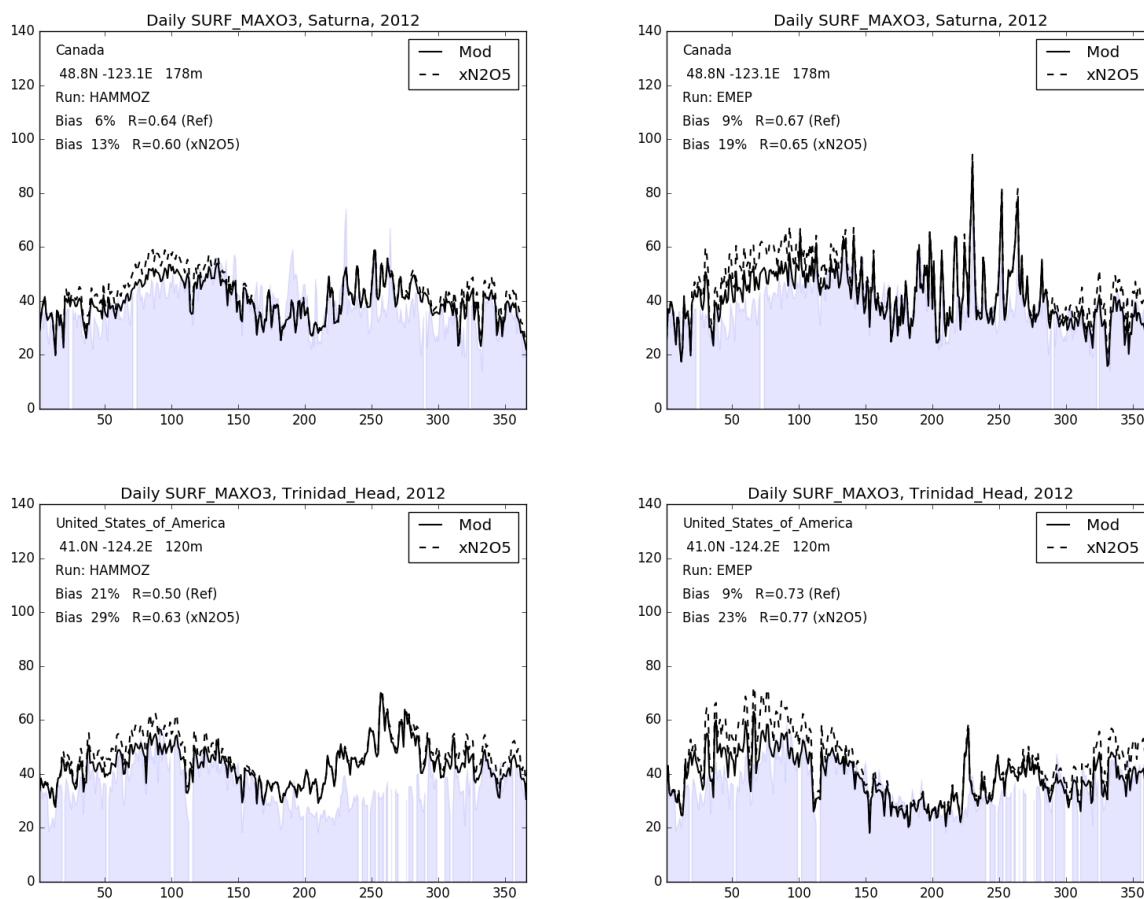


**Figure 6.** Modelled versus observed daily maximum ozone (ppbv) for two North American sites (Saturna, Canada, Trinidad Head, USA). The shaded area refers to surface station observations, the solid line is the reference run of the model and the dashed line the sensitivity run noN2O5 excluding heterogeneous  $\text{N}_2\text{O}_5$  reaction. On the upper left corner the station location, model, bias and correlation R are specified.

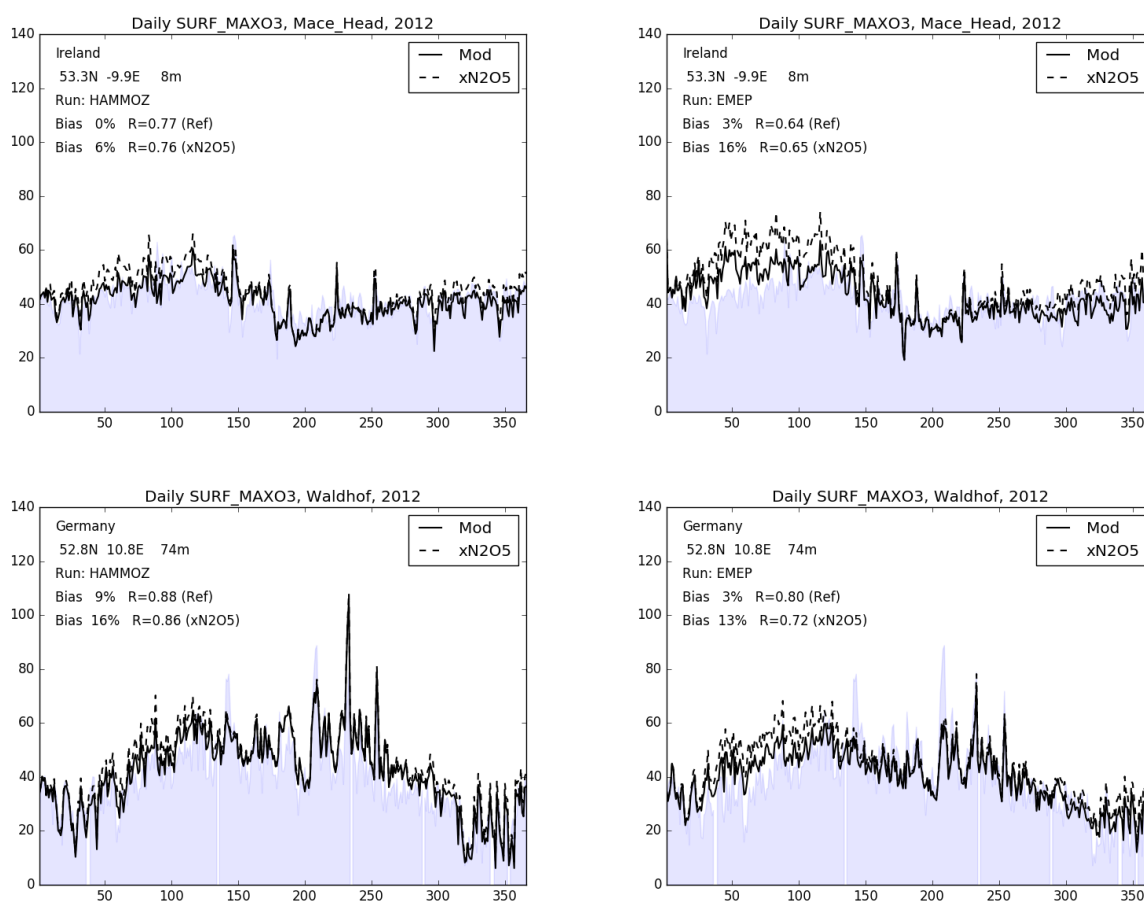


**Figure 7.** As Fig. 6 but for two European sites, Mace Head (Ireland) and Waldhof (Germany).

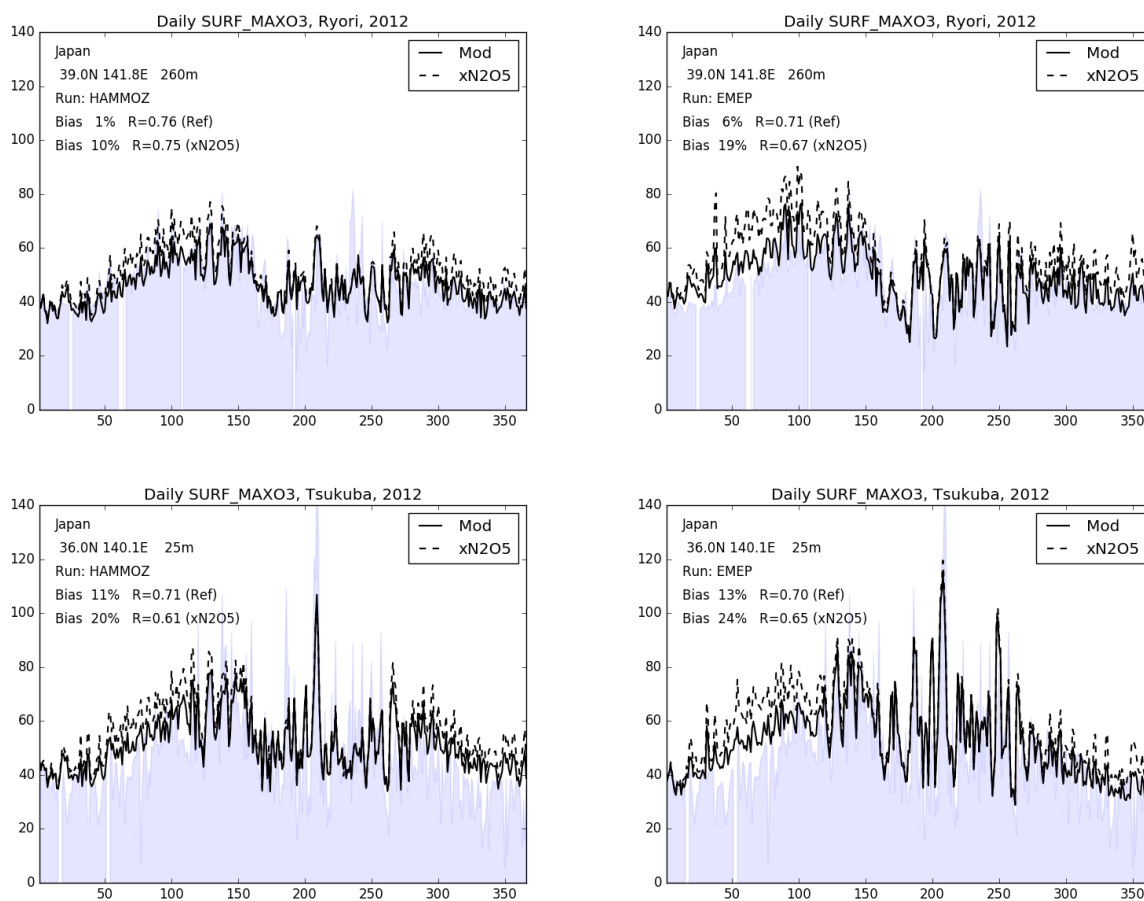


**Figure 8.** As Fig. 6 but for two Japanese sites, Ryori and Tsukuba.



## 6 Conclusions

- Two global transport models were used to investigate the implications of six heterogeneous (gas-aerosol uptake) reactions on ground-level ozone concentrations. Both models were harmonized to use similar parameterizations for most of these reactions, enabling us to compare the impacts of  $\text{N}_2\text{O}_5$ ,  $\text{NO}_3$ ,  $\text{NO}_2$ ,  $\text{O}_3$ ,  $\text{HNO}_3$ , and  $\text{HO}_2$  on ozone mixing ratios. Each reaction was evaluated systematically comparing the reference run to sensitivity simulations excluding one reaction at a time. Since heterogeneous reactions take place at the aerosol surface area, the modeled surface area density  $S_a$  of both models was compared to a satellite product retrieving the surface area. This comparison shows a good agreement in global pattern and especially the capability of both models to capture the extreme aerosol loadings in East Asia.
- The analysis of the sensitivity runs confirms that the globally most important heterogeneous reaction is the one of  $\text{N}_2\text{O}_5$ . This impact was expected from previous studies, with the surface reactions of  $\text{N}_2\text{O}_5$  having an impact on ozone mixing ratios through removal of reactive  $\text{NO}_x$  species. Some other heterogeneous reactions (especially the ones of  $\text{NO}_2$ ,  $\text{HO}_2$  and  $\text{HNO}_3$ ) gain some significance in highly polluted areas where aerosol surface areas are high, but the two models show quite different response in their response to these other gas-aerosol reactions. The EMEP model actually shows rather small impacts of these reactions, except in East and South Asia where some impacts can approach 10-20% of that of  $\text{N}_2\text{O}_5$ . ECHAM-HAMMOZ, on the other hand, shows quite marked responses to especially the  $\text{HNO}_3$  reactions. The reasons for this are related to differences in nitrate chemistry and surface area assumptions in the models, and to the differing spatial resolutions. It may well be that ECHAM-HAMMOZ overestimates the impact of  $\text{HNO}_3$  due to missing nitrate aerosol formation and EMEP underestimates the impact, due to the use of only coarse sea salt and dust aerosol for the  $\text{HNO}_3$  and  $\text{HO}_2$  reactions.

The reactions of  $\text{O}_3$  on dust and  $\text{NO}_3$  on aerosols were found to have only minor effects on ozone in comparison to the other reactions in both models. In terms of global spatial impact, all reactions related to nitrogen species alter atmospheric chemistry downwind of source areas to some extent, with changes being much larger in the polluted northern hemisphere than in the southern hemisphere.

Evaluation of the models with northern hemispheric ozone surface observations from the GAW/TOAR networks yields a better agreement of the models with observations in terms of daily maximum concentrations, variability and temporal correlations at most sites when the heterogeneous reactions are incorporated. The impacts of the  $\text{N}_2\text{O}_5$  reactions show strong seasonal variations, with biggest impacts in spring time when photochemical reactions are active and  $\text{N}_2\text{O}_5$  levels still high.

Due to lack of direct observations substantial uncertainties remain regarding the impact of heterogeneous reactions on tropospheric reactive gases. It should be noted, that neither model had an implementation of the particle-liquid-water/nitrate/chloride effects suggested by Bertram and Thornton (2009) and tested by e.g. Lowe et al. (2015). Further, neither model includes halogen chemistry, which is also known to impact  $\text{O}_3$  in polluted regions (e.g. Sarwar et al., 2014; Li et al., 2016). The large impact of  $\text{N}_2\text{O}_5$  seen in our work might be somewhat overestimated compared to that we would obtain if the chemistry of  $\text{ClNO}_2$  (which would recycle  $\text{NO}_x$ ) and other halogens could be included. Such improvements should result in better particle phase chemistry, and will be the subject of future work.





*Acknowledgements.* The authors wish to thank the Jülich Supercomputing Centre (2016) for providing the computing resources for the  
25 ECHAM-HAMMOZ simulations. The EMEP work was funded by the EU FP7 projects ECLAIRE (Project number 282910), and EMEP  
under UNECE, with computer time supported by the Research Council of Norway (Programme for Supercomputing). The project was also  
supported by the Swedish Climate Modelling Research Project MERGE. GAW surface ozone observation data were retrieved from the  
World Data Center for Greenhouse Gases in Tokyo, Japan. We acknowledge the substantial efforts of all data providers for making these  
measurements.

30 *Competing interests.* No competing interests are present



## References

- Aas, W., Tsyro, S., Bieber, E., Bergström, R., Ceburnis, D., Ellermann, T., Fagerli, H., Frölich, M., Gehrig, R., Makkonen, U., Nemitz, E., Otjes, R., Perez, N., Perrino, C., Prévôt, A. S. H., Putaud, J.-P., Simpson, D., Spindler, G., Vana, M., and Yttri, K. E.: Lessons learnt from the first EMEP intensive measurement periods, *Atmos. Chem. Physics*, 12, 8073–8094, doi:10.5194/acp-12-8073-2012, <http://www.atmos-chem-phys.net/12/8073/2012/>, 2012.
- Ainsworth, E. A., Yendrek, C. R., Sitch, S., Collins, W. J., and Emberson, L. D.: The Effects of Tropospheric Ozone on Net Primary Productivity and Implications for Climate Change, *Ann. Rev. Plant Biol.*, 63, 637–661, doi:10.1146/annurev-arplant-042110-103829, 2012.
- Ammann, M., Cox, R., Crowley, J., Jenkin, M., Mellouki, A., Rossi, M., Troe, J., and Wallington, T.: Evaluated kinetic and photochemical data for atmospheric chemistry: Volume VI–heterogeneous reactions with liquid substrates, *Atmospheric Chemistry and Physics*, 13, 8045–8228, 2013.
- Andersson-Sköld, Y. and Simpson, D.: Comparison of the chemical schemes of the EMEP MSC-W and the IVL photochemical trajectory models, *Atmos. Environ.*, 33, 1111–1129, 1999.
- Angelbratt, J., Mellqvist, J., Simpson, D., Jonson, J. E., Blumenstock, T., Borsdorff, T., Duchatelet, P., Forster, F., Hase, F., Mahieu, E., Notholt, J., Petersen, A. K., Raffalski, U., Servais, C., Sussman, R., and Warneke, T.: Carbon monoxide (CO) and ethane (C<sub>2</sub>H<sub>6</sub>) trends from ground-based solar FTIR measurements at six European stations, comparison and sensitivity analysis with the EMEP model, *Atmos. Chem. Physics*, 11, 9253–9269, doi:10.5194/acpd-11-13723-2011, <http://www.atmos-chem-phys-discuss.net/11/13723/2011/>, 2011.
- Arens, F., Gutzwiller, L., Baltensperger, U., Gaggeler, H. W., and Ammann, M.: Heterogeneous reaction of NO<sub>2</sub> on diesel soot particles, *Environmental science & technology*, 35, 2191–2199, 2001.
- Bauer, S., Balkanski, Y., Schulz, M., Hauglustaine, D., and Dentener, F.: Global modeling of heterogeneous chemistry on mineral aerosol surfaces: Influence on tropospheric ozone chemistry and comparison to observations, *Journal of Geophysical Research: Atmospheres* (1984–2012), 109, 2004.
- Bergström, R., Denier van der Gon, H. A. C., Prévôt, A. S. H., Yttri, K. E., and Simpson, D.: Modelling of organic aerosols over Europe (2002–2007) using a volatility basis set (VBS) framework: application of different assumptions regarding the formation of secondary organic aerosol, *Atmos. Chem. Physics*, 12, 8499–8527, doi:10.5194/acp-12-8499-2012, <http://www.atmos-chem-phys.net/12/8499/2012/>, 2012.
- Bertram, T. and Thornton, J.: Toward a general parameterization of N<sub>2</sub>O<sub>5</sub> reactivity on aqueous particles: the competing effects of particle liquid water, nitrate and chloride, *Atmospheric Chemistry and Physics*, 9, 8351–8363, 2009.
- Bian, H., Chin, M., Hauglustaine, D. A., Schulz, M., Myhre, G., Bauer, S. E., Lund, M. T., Karydis, V. A., Kucsera, T. L., Pan, X., Pozzer, A., Skeie, R. B., Steenrod, S. D., Sudo, K., Tsigaridis, K., Tsimpidi, A. P., and Tsyro, S. G.: Investigation of global nitrate from the AeroCom Phase III experiment, *Atmospheric Chemistry and Physics Discussions*, 2017, 1–44, doi:10.5194/acp-2017-359, <http://www.atmos-chem-phys-discuss.net/acp-2017-359/>, 2017.
- Binkowski, F. and Shankar, U.: The Regional Particulate Matter Model .1. Model description and preliminary results, *J. Geophys. Res.*, 100, 26 191–26 209, 1995.
- Brown, S. S. and Stutz, J.: Nighttime radical observations and chemistry, *Chem. Soc. Rev.*, 41, 6405–6447, doi:10.1039/C2CS35181A, <http://dx.doi.org/10.1039/C2CS35181A>, 2012.



- Brown, S. S., Dube, W. P., Fuchs, H., Ryerson, T. B., Wollny, A. G., Brock, C. A., Bahreini, R., Middlebrook, A. M., Neuman, J. A., Atlas, E., Roberts, J. M., Osthoff, H. D., Trainer, M., Fehsenfeld, F. C., and Ravishankara, A. R.: Reactive uptake coefficients for  $\text{N}_2\text{O}_5$  determined from aircraft measurements during the Second Texas Air Quality Study: Comparison to current model parameterizations, *J. Geophys. Res.*, 114, D00F10, doi:10.1029/2008JD011679, 2009.
- 35 Buseck, P. R. and Posfai, M.: Airborne minerals and related aerosol particles: Effects on climate and the environment, *Proceedings of the National Academy of Sciences*, 96, 3372–3379, 1999.
- Chang, W. L., Bhawe, P. V., Brown, S. S., Riemer, N., Stutz, J., and Dabdub, D.: Heterogeneous Atmospheric Chemistry, Ambient Measurements, and Model Calculations of  $\text{N}_2\text{O}_5$ : A Review, *Aerosol Science and Technology*, 45, 665–695, doi:10.1080/02786826.2010.551672, <http://www.tandfonline.com/doi/abs/10.1080/02786826.2010.551672>, 2011a.
- Chang, W. L., Bhawe, P. V., Brown, S. S., Riemer, N., Stutz, J., and Dabdub, D.: Heterogeneous atmospheric chemistry, ambient measurements, and model calculations of  $\text{N}_2\text{O}_5$ : A review, *Aerosol Science and Technology*, 45, 665–695, 2011b.
- Crutzen, P., Lawrence, M., and Poschl, U.: On the background photochemistry of tropospheric ozone, 51, 123–146, international Symposium to Commemorate the 100th Anniversary of the Birth of Carl Gustaf Rossby (Rossby-100), STOCKHOLM, SWEDEN, JUN 08-12, 1998, 1999.
- 5 Davies, J. A. and Cox, R. A.: Kinetics of the heterogeneous reaction of  $\text{HNO}_3$  with NaCl: Effect of water vapor, *The Journal of Physical Chemistry A*, 102, 7631–7642, 1998.
- Davis, J., Bhawe, P., and Foley, K.: Parameterization of  $\text{N}_2\text{O}_5$  reaction probabilities on the surface of particles containing ammonium, sulfate, and nitrate, *Atmospheric Chemistry and Physics*, 8, 5295–5311, 2008.
- 10 Dentener, F. J. and Crutzen, P. J.: Reaction of  $\text{N}_2\text{O}_5$  on tropospheric aerosols: Impact on the global distributions of  $\text{NO}_x$ ,  $\text{O}_3$ , and OH, *Journal of Geophysical Research: Atmospheres* (1984–2012), 98, 7149–7163, 1993.
- Emmons, L., Walters, S., Hess, P., Lamarque, J.-F., Pfister, G., Fillmore, D., Granier, C., Guenther, A., Kinnison, D., Laepple, T., et al.: Description and evaluation of the Model for Ozone and Related chemical Tracers, version 4 (MOZART-4), *Geoscientific Model Development*, 3, 43–67, 2010.
- 15 Evans, M. and Jacob, D. J.: Impact of new laboratory studies of  $\text{N}_2\text{O}_5$  hydrolysis on global model budgets of tropospheric nitrogen oxides, ozone, and OH, *Geophysical Research Letters*, 32, 2005.
- Fagerli, H. and Aas, W.: Trends of nitrogen in air and precipitation: Model results and observations at EMEP sites in Europe, 1980-2003, *Environ. Poll.*, 154, 448–461, 2008.
- 20 Fairlie, T. D., Jacob, D. J., Dibb, J. E., Alexander, B., Avery, M. A., Donkelaar, A. v., and Zhang, L.: Impact of mineral dust on nitrate, sulfate, and ozone in transpacific Asian pollution plumes, *Atmospheric Chemistry and Physics*, 10, 3999–4012, 2010.
- Fiore, A., Dentener, F., Wild, O., Cuvelier, C., Schultz, M., Hess, P., Textor, C., Schulz, M., Doherty, R., Horowitz, L., et al.: Multimodel estimates of intercontinental source-receptor relationships for ozone pollution, *Journal of Geophysical Research: Atmospheres* (1984–2012), 114, 2009.
- 25 Frenzel, A., Scheer, V., Sikorski, R., George, C., Behnke, W., and Zetzsch, C.: Heterogeneous Interconversion Reactions of  $\text{BrNO}_2$ ,  $\text{ClNO}_2$ ,  $\text{Br}_2$ , and  $\text{Cl}_2$ , *The Journal of Physical Chemistry A*, 102, 1329–1337, doi:10.1021/jp973044b, <http://dx.doi.org/10.1021/jp973044b>, 1998.
- Gauss, M., Benedictow, A., and Hjellbrekke, A.-G.: Photo-oxidants: validation and combined maps, Supplementary material to emep status report 1/2011, available online at [www.emep.int](http://www.emep.int), The Norwegian Meteorological Institute, Oslo, Norway, 2011.
- George, C., Ammann, M., D’Anna, B., Donaldson, D., and Nizkorodov, S. A.: Heterogeneous Photochemistry in the Atmosphere, *Chemical reviews*, 2015.
- 30



- George, I., Matthews, P., Whalley, L., Brooks, B., Goddard, A., Baeza-Romero, M., and Heard, D.: Measurements of uptake coefficients for heterogeneous loss of HO<sub>2</sub> onto submicron inorganic salt aerosols, *Physical Chemistry Chemical Physics*, 15, 12 829–12 845, 2013.
- Gerber, H. E.: Relative-Humidity Parameterization of the Navy Aerosol Model (NAM), NRL Report 8956, Naval Research Laboratory, Washington, DC, 1985.
- 35 Goodman, A., Underwood, G., and Grassian, V.: Heterogeneous reaction of NO<sub>2</sub>: Characterization of gas-phase and adsorbed products from the reaction, 2 NO<sub>2</sub> (g)+ H<sub>2</sub>O (a) → HONO (g)+ HNO<sub>3</sub> (a) on hydrated silica particles, *The Journal of Physical Chemistry A*, 103, 7217–7223, 1999.
- Grewe, V., Brunner, D., Dameris, M., Grenfell, J., Hein, R., Shindell, D., and Staehelin, J.: Origin and variability of upper tropospheric nitrogen oxides and ozone at northern mid-latitudes, *Atmospheric Environment*, 35, 3421–3433, 2001.
- Griffiths, P. T., Badger, C. L., Cox, R. A., Folkers, M., Henk, H. H., and Mentel, T. F.: Reactive uptake of N<sub>2</sub>O<sub>5</sub> by aerosols containing dicarboxylic acids. Effect of particle phase, composition, and nitrate content, *The Journal of Physical Chemistry A*, 113, 5082–5090, 2009.
- 5 Gross, S., Iannone, R., Xiao, S., and Bertram, A. K.: Reactive uptake studies of NO<sub>3</sub> and N<sub>2</sub>O<sub>5</sub> on alkenoic acid, alkanoate, and polyalcohol substrates to probe nighttime aerosol chemistry, *Physical Chemistry Chemical Physics*, 11, 7792–7803, 2009.
- Guenther, A., Karl, T., Harley, P., Wiedinmyer, C., Palmer, P., and Geron, C.: Estimates of global terrestrial isoprene emissions using MEGAN (Model of Emissions of Gases and Aerosols from Nature), *Atmospheric Chemistry and Physics Discussions*, 6, 107–173, 2006.
- Hallquist, M., Wenger, J., Baltensperger, U., Rudich, Y., Simpson, D., Claeys, M., Dommen, J., Donahue, N., George, C., Goldstein, A., et al.:  
10 The formation, properties and impact of secondary organic aerosol: current and emerging issues, *Atmospheric Chemistry and Physics*, 9, 5155–5236, 2009.
- Hanisch, F. and Crowley, J. N.: The heterogeneous reactivity of gaseous nitric acid on authentic mineral dust samples, and on individual mineral and clay mineral components, *Physical Chemistry Chemical Physics*, 3, 2474–2482, 2001.
- Harrison, R. M. and Collins, G. M.: Measurements of reaction coefficients of NO<sub>2</sub> and HONO on aerosol particles, *Journal of atmospheric  
15 chemistry*, 30, 397–406, 1998.
- Harrison, R. M. and Yin, J.: Particulate matter in the atmosphere: which particle properties are important for its effects on health?, *Science of the total environment*, 249, 85–101, 2000.
- Hauglustaine, D., Balkanski, Y., and Schulz, M.: A global model simulation of present and future nitrate aerosols and their direct radiative forcing of climate., *Atmospheric Chemistry & Physics*, 14, 2014.
- 20 Henrot, A.-J., Stanelle, T., Schröder, S., Siegenthaler, C., Taraborrelli, D., and Schultz, M.: Implementation of the biogenic emission model MEGAN (v2. 1) into the ECHAM6-HAMMOZ chemistry climate model, *Geoscientific Model Development [= GMD]*, 2017.
- Hodzic, A., Bessagnet, B., and Vautard, R.: A model evaluation of coarse-mode nitrate heterogeneous formation on dust particles, *Atmospheric Environment*, 40, 4158–4171, 2006.
- Huijnen, V., Williams, J., and Flemming, J.: Modeling global impacts of heterogeneous loss of HO<sub>2</sub> on cloud droplets, ice particles and  
25 aerosols, *Atmospheric Chemistry and Physics Discussions*, 14, 8575–8632, 2014.
- IPCC: Annex I: Atlas of Global and Regional Climate Projections, book section AI, pp. 1311–1394, Cambridge University Press, Cambridge, United Kingdom and New York, NY, USA, doi:10.1017/CBO9781107415324.029, [www.climatechange2013.org](http://www.climatechange2013.org), 2013.
- Jacob, D. J.: Heterogeneous chemistry and tropospheric ozone, *Atmospheric Environment*, 34, 2131–2159, 2000.
- Jonson, J., Stohl, A., Fiore, A., Hess, P., Szopa, S., Wild, O., Zeng, G., Dentener, F., Lupu, A., Schultz, M., Duncan, B., Sudo, K., Wind, P.,  
30 Schulz, M., Marmer, E., Cuvelier, C., Keating, T., Zuber, A., Valdebenito, A., Dorokhov, V., De Backer, H., Davies, J., Chen, G., Johnson,



- B., Tarasick, D., Stübi, R., Newchurch, M., von der Gathen, P., Steinbrecht, W., and Claude, H.: A multi-model analysis of vertical ozone profiles, *Atmos. Chem. Physics*, 10, 5759–5783, doi:10.5194/acp-10-5759-2010, 2010.
- Jonson, J. E., Semeena, V. S., and Simpson, D.: Global ozone bias, in: Transboundary particulate matter, photo-oxidants, acidifying and eutrophying components. Status Report 1/2015, pp. 115–128, The Norwegian Meteorological Institute, Oslo, Norway, 2015.
- 35 Jülich Supercomputing Centre: JURECA: General-purpose supercomputer at Jülich Supercomputing Centre, *Journal of large-scale research facilities*, 2, doi:10.17815/jlsrf-2-121, <http://dx.doi.org/10.17815/jlsrf-2-121>, 2016.
- Kinnison, D., Brasseur, G., Walters, S., Garcia, R., Marsh, D., Sassi, F., Harvey, V., Randall, C., Emmons, L., Lamarque, J., et al.: Sensitivity of chemical tracers to meteorological parameters in the MOZART-3 chemical transport model, *Journal of Geophysical Research: Atmospheres* (1984–2012), 112, 2007.
- Kleffmann, J., Becker, K., and Wiesen, P.: Heterogeneous NO<sub>2</sub> conversion processes on acid surfaces: possible atmospheric implications, *Atmospheric Environment*, 32, 2721–2729, 1998.
- Lamarque, J., Emmons, L., Hess, P., Kinnison, D. E., Tilmes, S., Vitt, F., Heald, C., Holland, E. A., Lauritzen, P., Neu, J., et al.: CAM-chem:  
5 Description and evaluation of interactive atmospheric chemistry in the Community Earth System Model, *Geosci. Model Dev*, 5, 369–411, 2012.
- Li, Q., Zhang, L., Wang, T., Tham, Y. J., Ahmadov, R., Xue, L., Zhang, Q., and Zheng, J.: Impacts of heterogeneous uptake of dinitrogen pentoxide and chlorine activation on ozone and reactive nitrogen partitioning: improvement and application of the WRF-Chem model in southern China, *Atmos. Chem. Physics*, 16, 14 875–14 890, doi:10.5194/acp-16-14875-2016, 2016.
- 10 Liao, H. and Seinfeld, J. H.: Global impacts of gas-phase chemistry-aerosol interactions on direct radiative forcing by anthropogenic aerosols and ozone, *Journal of Geophysical Research: Atmospheres* (1984–2012), 110, 2005.
- Liu, Y., Gibson, E. R., Cain, J. P., Wang, H., Grassian, V. H., and Laskin, A.: Kinetics of heterogeneous reaction of CaCO<sub>3</sub> particles with gaseous HNO<sub>3</sub> over a wide range of humidity, *The Journal of Physical Chemistry A*, 112, 1561–1571, 2008.
- Lowe, D., Archer-Nicholls, S., Morgan, W., Allan, J., Utembe, S., Ouyang, B., Aruffo, E., Le Breton, M., Zaveri, R. A., Di Carlo, P., Percival,  
15 C., Coe, H., Jones, R., and McFiggans, G.: WRF-Chem model predictions of the regional impacts of N<sub>2</sub>O<sub>5</sub> heterogeneous processes on night-time chemistry over north-western Europe, *Atmos. Chem. Physics*, 15, 1385–1409, doi:10.5194/acp-15-1385-2015, 2015.
- Lowe, D., Ryder, J., Leigh, R., Dorsey, J. R., and McFiggans, G.: Modelling multi-phase halogen chemistry in the coastal marine boundary layer: investigation of the relative importance of local chemistry vs. long-range transport, *Atmos. Chem. Physics*, 11, 979–994, doi:10.5194/acp-11-979-2011, 2011.
- 20 Macintyre, H. and Evans, M.: Sensitivity of a global model to the uptake of N<sub>2</sub>O<sub>5</sub> by tropospheric aerosol, *Atmospheric Chemistry and Physics*, 10, 7409–7414, 2010.
- Mao, J., Fan, S., Jacob, D. J., and Travis, K. R.: Radical loss in the atmosphere from Cu-Fe redox coupling in aerosols, *Atmospheric Chemistry and Physics*, 13, 509–519, 2013.
- Mogili, P. K., Kleiber, P. D., Young, M. A., and Grassian, V. H.: Heterogeneous uptake of ozone on reactive components of mineral dust  
25 aerosol: An environmental aerosol reaction chamber study, *The Journal of Physical Chemistry A*, 110, 13 799–13 807, 2006.
- Moise, T., Talukdar, R., Frost, G., Fox, R., and Rudich, Y.: Reactive uptake of NO<sub>3</sub> by liquid and frozen organics, *Journal of Geophysical Research: Atmospheres* (1984–2012), 107, AAC–6, 2002.
- Morgan, W. T., Ouyang, B., Allan, J. D., Aruffo, E., Di Carlo, P., Kennedy, O. J., Lowe, D., Flynn, M. J., Rosenberg, P. D., Williams, P. I., Jones, R., McFiggans, G. B., and Coe, H.: Influence of aerosol chemical composition on N<sub>2</sub>O<sub>5</sub> uptake: airborne regional measurements  
30 in northwestern Europe, *Atmospheric Chemistry and Physics*, 15, 973–990, doi:10.5194/acp-15-973-2015, 2015.



- Mozurkewich, M. and Calvert, J. G.: Reaction possibility of  $\text{N}_2\text{O}_5$  on aqueous aerosols, *Journal of Geophysical Research: Atmospheres*, 93, 15,889–15,896, 1988.
- Neubauer, D., Siegenthaler-Le Drian, C., Ferrachat, S., Bey, I., Lohmann, U., Stanelle, T., Frontoso, G., Stier, P., Schutgens, N., Schmidt, H., Rast, S., Schultz, M. G., Schroeder, S., Tegen, I., and Heinold, B.: The new version of the global aerosol-climate model ECHAM6-HAM: aerosol evaluation against observations and previous versions, Special Issue Global Model Development and Atmospheric Chemistry and Physics, in preparation.
- Nicolas, M., Ndour, M., Ka, O., D'Anna, B., and George, C.: Photochemistry of atmospheric dust: ozone decomposition on illuminated titanium dioxide, *Environmental science & technology*, 43, 7437–7442, 2009.
- Parrish, D., Millet, D., and Goldstein, A.: Increasing ozone in marine boundary layer inflow at the west coasts of North America and Europe, *Atmospheric Chemistry and Physics*, 9, 1303–1323, 2009.
- Parrish, D., Lamarque, J.-F., Naik, V., Horowitz, L., Shindell, D., Staehelin, J., Derwent, R., Cooper, O., Tanimoto, H., Volz-Thomas, A., et al.: Long-term changes in lower tropospheric baseline ozone concentrations: Comparing chemistry-climate models and observations at northern midlatitudes, *Journal of Geophysical Research: Atmospheres*, 119, 5719–5736, 2014.
- Pathak, R., Wu, W., and Wang, T.: Summertime  $\text{PM}_{2.5}$  ionic species in four major cities of China: nitrate formation in an ammonia-deficient atmosphere, *Atmospheric Chemistry and Physics*, 9, 1711–1722, 2009.
- Pathak, R. K., Wu, W. S., and Wang, T.: Summertime  $\text{PM}_{2.5}$  ionic species in four major cities of China: nitrate formation in an ammonia-deficient atmosphere, *Atmospheric Chemistry and Physics Discussions*, 8, 11 487–11 517, 2008.
- Platt, U., Perner, D., Harris, G., Winer, A., and Pitts, J. j.: Observations of nitrous acid in an urban atmosphere by differential optical absorption, *Nature*, 285, 312–314, 1980.
- Pöschl, U.: Atmospheric aerosols: composition, transformation, climate and health effects, *Angewandte Chemie International Edition*, 44, 7520–7540, 2005.
- Remorov, R., Gershenzon, Y. M., Molina, L., and Molina, M.: Kinetics and mechanism of  $\text{HO}_2$  uptake on solid NaCl, *The Journal of Physical Chemistry A*, 106, 4558–4565, 2002.
- Reus, M., Dentener, F., Thomas, A., Borrmann, S., Ström, J., and Lelieveld, J.: Airborne observations of dust aerosol over the North Atlantic Ocean during ACE 2: Indications for heterogeneous ozone destruction, *Journal of Geophysical Research: Atmospheres* (1984–2012), 105, 15 263–15 275, 2000.
- Riedel, T., Bertram, T., Ryder, O., Liu, S., Day, D., Russell, L., Gaston, C., Prather, K., and Thornton, J.: Direct  $\text{N}_2\text{O}_5$  reactivity measurements at a polluted coastal site, *Atmospheric Chemistry and Physics*, 12, 2959–2968, 2012.
- Rierner, N., Vogel, H., Vogel, B., Schell, B., Ackermann, I., Kessler, C., and Hass, H.: Impact of the heterogeneous hydrolysis of  $\text{N}_2\text{O}_5$  on chemistry and nitrate formation in the lower troposphere under photochemical conditions, *J. Geophys. Res.*, 108, 4144, doi:10.1029/2002JD002436, 2003a.
- Rierner, N., Vogel, H., Vogel, B., Schell, B., Ackermann, I., Kessler, C., and Hass, H.: Impact of the heterogeneous hydrolysis of  $\text{N}_2\text{O}_5$  on chemistry and nitrate aerosol formation in the lower troposphere under photochemical conditions, *Journal of Geophysical Research: Atmospheres* (1984–2012), 108, 2003b.
- Rierner, N., Vogel, H., Vogel, B., Anttila, T., Kiendler-Scharr, A., and Mentel, T.: Relative importance of organic coatings for the heterogeneous hydrolysis of  $\text{N}_2\text{O}_5$  during summer in Europe, *Journal of Geophysical Research: Atmospheres* (1984–2012), 114, 2009.
- Rudich, Y., Talukdar, R. K., Ravishankara, A., and Fox, R.: Reactive uptake of  $\text{NO}_3$  on pure water and ionic solutions, *Journal of Geophysical Research: Atmospheres* (1984–2012), 101, 21 023–21 031, 1996.





- Rudich, Y., Talukdar, R., and Ravishankara, A.: Multiphase chemistry of  $\text{NO}_3$  in the remote troposphere, *Journal of Geophysical Research: Atmospheres* (1984–2012), 103, 16 133–16 143, 1998.
- Saathoff, H., Naumann, K.-H., Riemer, N., Kamm, S., Möhler, O., Schurath, U., Vogel, H., and Vogel, B.: The loss of  $\text{NO}_2$ ,  $\text{HNO}_3$ ,  $\text{NO}_3/\text{N}_2\text{O}_5$ , and  $\text{HO}_2/\text{HOONO}_2$  on soot aerosol: A chamber and modeling study, *Geophysical Research Letters*, 28, 1957–1960, 2001.
- 35 Sander, S. P., Friedl, R., Golden, D., Kurylo, M., Moortgat, G., Keller-Rudek, H., Wine, P., Ravishankara, A., Kolb, C., Molina, M., et al.: Chemical kinetics and photochemical data for use in atmospheric studies: evaluation number 15, National Aeronautics and Space Administration, Jet Propulsion Laboratory, California Institute of Technology Pasadena, CA, 2006.
- Sarwar, G., Simon, H., Xing, J., and Mathur, R.: Importance of tropospheric  $\text{ClNO}_2$  chemistry across the Northern Hemisphere, *Geophys. Res. Lett.*, 41, 4050–4058, doi:10.1002/2014GL059962, 2014.
- Schaap, M., Cuvelier, C., Hendriks, C., Bessagnet, B., Baldasano, J., Colette, A., Thunis, P., Karam, D., Fagerli, H., Graff, A.,  
5 Kranenburg, R., Nyiri, A., Pay, M., RouÅ¹l, L., Schulz, M., Simpson, D., Stern, R., Terrenoire, E., and Wind, P.: Performance of European chemistry transport models as function of horizontal resolution, *Atmospheric Environment*, 112, 90 – 105, doi:<http://dx.doi.org/10.1016/j.atmosenv.2015.04.003>, <http://www.sciencedirect.com/science/article/pii/S1352231015300066>, 2015.
- Schultz, M., H. A., Bottenheim, J., Buchmann, B., Galbally, I., Gilge, S., and et al.,.: The Global Atmosphere Watch reactive gases measurement network, *Elem Sci Anth.*, 3, doi:<http://doi.org/10.12952/journal.elementa.000067>, 2015.
- 10 Schultz, M., Schroeder, S., Lyapina, O., and Cooper, O.: Tropospheric Ozone Assessment Report: Database and metrics data of global surface ozone observations., 2017.
- Schultz, M. G., Stadtler, S., Schroeder, S., Taraborrelli, D., Henrot, A., Kaffashzadeh, N., Franco, B., Ferrachat, S., Siegenthaler-Le Drian, C., Lohmann, U., Neubauer, D., Wahl, S., Kokkola, H., Kuehn, T., Stier, P., Kinnison, D., Tyndall, G., and Orlando, J.: The Chemistry Climate Model ECHAM-HAMMOZ, Global Model Development, in preparation.
- 15 Schwartz, S. E.: Mass-transport considerations pertinent to aqueous phase reactions of gases in liquid-water clouds, in: *Chemistry of multiphase atmospheric systems*, pp. 415–471, Springer, 1986.
- Seinfeld, J. H. and Pandis, S. N.: *Atmospheric chemistry and physics: from air pollution to climate change*, John Wiley & Sons, 2012.
- Sillman, S., Logan, J., and Wofsy, S.: The sensitivity of ozone to nitrogen oxides and hydrocarbons in regional ozone episodes, *J. Geophys. Res.*, 95, 1837–1851, 1990.
- 20 Simpson, D., Winiwarer, W., Börjesson, G., Cinderby, S., Ferreira, A., Guenther, A., Hewitt, C. N., Janson, R., Khalil, M. A. K., Owen, S., Pierce, T. E., Puxbaum, H., Shearer, M., Skiba, U., Steinbrecher, R., Tarrasón, L., and Öquist, M. G.: Inventorying emissions from Nature in Europe, *J. Geophys. Res.*, 104, 8113–8152, 1999.
- Simpson, D., Butterbach-Bahl, K., Fagerli, H., Kesik, M., Skiba, U., and Tang, S.: Deposition and Emissions of Reactive Nitrogen over European Forests: A Modelling Study, *Atmos. Environ.*, 40, 5712–5726, doi:10.1016/j.atmosenv.2006.04.063, 2006a.
- 25 Simpson, D., Fagerli, H., Hellsten, S., Knulst, J., and Westling, O.: Comparison of modelled and monitored deposition fluxes of sulphur and nitrogen to ICP-forest sites in Europe, *Biogeosciences*, 3, 337–355, 2006b.
- Simpson, D., Benedictow, A., Berge, H., Bergström, R., Emberson, L. D., Fagerli, H., Flechard, C. R., Hayman, G. D., Gauss, M., Jonson, J. E., Jenkin, M. E., Nyiri, A., Richter, C., Semeena, V. S., Tsyro, S., Tuovinen, J.-P., Valdebenito, A., and Wind, P.: The EMEP MSC-W chemical transport model – technical description, *Atmos. Chem. Physics*, 12, 7825–7865, doi:10.5194/acp-12-7825-2012, <http://www.atmos-chem-phys.net/12/7825/2012/acp-12-7825-2012.html>, 2012.
- 30



- Simpson, D., Arneth, A., Mills, G., Solberg, S., and Uddling, J.: Ozone - the persistent menace; interactions with the N cycle and climate change, *Current Op. Environ. Sust.*, 9-10, 9–19, doi:<http://dx.doi.org/10.1016/j.cosust.2014.07.008>, sI: System dynamics and sustainability, 2014.
- Simpson, D., Tsyro, S., and Wind, P.: Updates to the EMEP/MSC-W model, in: Transboundary particulate matter, photo-oxidants, acidifying and eutrophying components. Status Report 1/2015, pp. 129–138, The Norwegian Meteorological Institute, Oslo, Norway, 2015.
- 35 Simpson, D., Bergström, R., Denby, B., Wind, P., and Others, X.: Updates to the EMEP/MSC-W model, 2016–2017, in: Transboundary particulate matter, photo-oxidants, acidifying and eutrophying components. EMEP Status Report 1/2016, p. xx, The Norwegian Meteorological Institute, Oslo, Norway, 2017.
- Solomon, S.: Stratospheric ozone depletion: A review of concepts and history, *Reviews of Geophysics-Richmond Virginia Washington*, 37, 275–316, 1999.
- Stadtler, S.: Heterogeneous  $\text{N}_2\text{O}_5$  Chemistry in the Aerosol-Chemistry-Climate Model ECHAM6-HAMMOZ, Master's thesis, University of Bonn, 2015.
- 5 Stein, O., Flemming, J., Inness, A., Kaiser, J. W., and Schultz, M. G.: Global reactive gases forecasts and reanalysis in the MACC project, *Journal of Integrative Environmental Sciences*, 9, 57–70, 2012.
- Stevens, B., Giorgetta, M., Esch, M., Mauritsen, T., Crueger, T., Rast, S., Salzmann, M., Schmidt, H., Bader, J., Block, K., et al.: Atmospheric component of the MPI-M Earth System Model: ECHAM6, *Journal of Advances in Modeling Earth Systems*, 5, 146–172, 2013.
- Stone, D., Evans, M. J., Walker, H., Ingham, T., Vaughan, S., Ouyang, B., Kennedy, O. J., McLeod, M. W., Jones, R. L., Hopkins, J., Punjabi, S., Lidster, R., Hamilton, J. F., Lee, J. D., Lewis, A. C., Carpenter, L. J., Forster, G., Oram, D. E., Reeves, C. E., Bauguutte, S., Morgan, W., Coe, H., Aruffo, E., Dari-Salisburgo, C., Giammaria, F., Di Carlo, P., and Heard, D. E.: Radical chemistry at night: comparisons between observed and modelled HO<sub>x</sub>, NO<sub>3</sub> and N<sub>2</sub>O<sub>5</sub> during the RONOCO project, *Atmospheric Chemistry and Physics*, 14, 1299–1321, doi:10.5194/acp-14-1299-2014, 2014.
- 10 Taketani, F., Kanaya, Y., and Akimoto, H.: Kinetics of heterogeneous reactions of HO<sub>2</sub> radical at ambient concentration levels with (NH<sub>4</sub>)<sub>2</sub>SO<sub>4</sub> and NaCl aerosol particles, *The Journal of Physical Chemistry A*, 112, 2370–2377, 2008.
- 15 Taraborrelli, D., Lawrence, M., Butler, T., Sander, R., and Lelieveld, J.: Mainz Isoprene Mechanism 2 (MIM2): an isoprene oxidation mechanism for regional and global atmospheric modelling, *Atmospheric Chemistry and Physics*, 9, 2751–2777, 2009.
- Thornton, J. and Abbatt, J. P.: Measurements of HO<sub>2</sub> uptake to aqueous aerosol: Mass accommodation coefficients and net reactive loss, *Journal of Geophysical Research: Atmospheres* (1984–2012), 110, 2005.
- 20 Thornton, J. A., Braban, C. F., and Abbatt, J. P.: N<sub>2</sub>O<sub>5</sub> hydrolysis on sub-micron organic aerosols: the effect of relative humidity, particle phase, and particle size, *Physical Chemistry Chemical Physics*, 5, 4593–4603, 2003.
- Thornton, J. A., Jaeglé, L., and McNeill, V. F.: Assessing known pathways for HO<sub>2</sub> loss in aqueous atmospheric aerosols: Regional and global impacts on tropospheric oxidants, *Journal of Geophysical Research: Atmospheres* (1984–2012), 113, 2008.
- Tilgner, A., Majdik, Z., Sehili, A., Simmel, M., Wolke, R., and Herrmann, H.: SPACCIM: Simulations of the multiphase chemistry occurring in the FEBUKO hill cap cloud experiments, *Atmospheric Environment*, 39, 4389–4401, 2005.
- 25 Tsyro, S., Aas, W., Soares, J., Sofiev, M., Berge, H., and Spindler, G.: Modelling of sea salt concentrations over Europe: key uncertainties and comparison with observations, *Atmos. Chem. Physics*, 11, 10 367–10 388, doi:10.5194/acp-11-10367-2011, <http://www.atmos-chem-phys.net/11/10367/2011/>, 2011.
- Underwood, G., Song, C., Phadnis, M., Carmichael, G., and Grassian, V.: Heterogeneous reactions of NO<sub>2</sub> and HNO<sub>3</sub> on oxides and mineral dust: A combined laboratory and modeling study, *Journal of Geophysical Research: Atmospheres* (1984–2012), 106, 18 055–18 066, 2001.
- 30



- Usher, C. R., Michel, A. E., and Grassian, V. H.: Reactions on mineral dust, *Chemical reviews*, 103, 4883–4940, 2003.
- van Donkelaar, A., Martin, R. V., Brauer, M., and Boys, B. L.: Use of satellite observations for long-term exposure assessment of global concentrations of fine particulate matter, *Environmental health perspectives*, 123, 135, 2015.
- Van Vuuren, D. P., Edmonds, J., Kainuma, M., Riahi, K., Thomson, A., Hibbard, K., Hurtt, G. C., Kram, T., Krey, V., Lamarque, J.-F., et al.:  
35 The representative concentration pathways: an overview, *Climatic change*, 109, 5, 2011.
- Verwer, J. and Simpson, D.: Explicit methods for stiff ODEs from atmospheric chemistry, *Applied Numerical Mathematics*, 18, 413–430, 1995.
- Verwer, J. G., Blom, J. G., Van Loon, M., and Spee, E. J.: A comparison of stiff ODE solvers for atmospheric chemistry problems, *Atmos. Environ.*, 30, 49–58, 1996.
- 695 Vieno, M., Dore, A. J., Bealey, W. J., Stevenson, D. S., and Sutton, M. A.: The importance of source configuration in quantifying footprints of regional atmospheric sulphur deposition, *Science of the Total Environment*, 408, 985–995, doi:10.1016/j.scitotenv.2009.10.048, 2010.
- Vieno, M., Heal, M. R., Hallsworth, S., Famulari, D., Doherty, R. M., Dore, A. J., Tang, Y. S., Braban, C. F., Leaver, D., Sutton, M. A., and Reis, S.: The role of long-range transport and domestic emissions in determining atmospheric secondary inorganic particle concentrations across the UK, *Atmos. Chem. Physics*, 14, 8435–8447, doi:10.5194/acp-14-8435-2014, <http://www.atmos-chem-phys.net/14/8435/2014/>,  
700 2014.
- Vignati, E., Wilson, J., and Stier, P.: M7: An efficient size-resolved aerosol microphysics module for large-scale aerosol transport models, *Journal of Geophysical Research: Atmospheres* (1984–2012), 109, 2004.
- Vinken, G. C. M., Boersma, K. F., Jacob, D. J., and Meijer, E. W.: Accounting for non-linear chemistry of ship plumes in the GEOS-Chem global chemistry transport model, *Atmos. Chem. Physics*, 11, 11 707–11 722, doi:10.5194/acp-11-11707-2011, <http://www.atmos-chem-phys.net/11/11707/2011/>, 2011.  
705
- von Glasow, R., Lawrence, M. G., Sander, R., and Crutzen, P. J.: Modeling the chemical effects of ship exhaust in the cloud-free marine boundary layer, *Atmos. Chem. Physics*, 3, 233–250, <http://www.atmos-chem-phys.net/3/233/2003/>, 2003.
- Wagner, N., Riedel, T., Young, C., Bahreini, R., Brock, C., Dubé, W., Kim, S., Middlebrook, A., Öztürk, F., Roberts, J., et al.: N<sub>2</sub>O<sub>5</sub> uptake coefficients and nocturnal NO<sub>2</sub> removal rates determined from ambient wintertime measurements, *Journal of Geophysical Research: Atmospheres*, 118, 9331–9350, 2013.  
710
- Wahner, A., Mentel, T. F., Sohn, M., and Stier, J.: Heterogeneous reaction of N<sub>2</sub>O<sub>5</sub> on sodium nitrate aerosol, *Journal of Geophysical Research: Atmospheres* (1984–2012), 103, 31 103–31 112, 1998.
- Whalley, L., Stone, D., George, I., Mertes, S., van Pinxteren, D., Tilgner, A., Herrmann, H., Evans, M., and Heard, D.: The influence of clouds on radical concentrations: observations and modelling studies of HO<sub>x</sub> during the Hill Cap Cloud Thuringia (HCCT) campaign in  
715 2010, *Atmospheric Chemistry and Physics*, 15, 3289–3301, 2015.
- Wild, O. and Akimoto, H.: Intercontinental transport of ozone and its precursors in a three-dimensional global CTM, *Journal of Geophysical Research: Atmospheres*, 106, 27 729–27 744, 2001.
- Yang, X., Pyle, J. A., and Cox, R. A.: Sea salt aerosol production and bromine release: Role of snow on sea ice, *Geophysical Research Letters*, 35, 2008.
- 720 Zhang, K., O'donnell, D., Kazil, J., Stier, P., Kinne, S., Lohmann, U., Ferrachat, S., Croft, B., Quaas, J., Wan, H., et al.: The global aerosol-climate model ECHAM-HAM, version 2: sensitivity to improvements in process representations, *Atmospheric Chemistry and Physics*, 12, 8911–8949, 2012.